Prediction of self-diffusion coefficient and shear viscosity of water and its binary mixtures with methanol and ethanol by molecular simulation

Gabriela Guevara-Carrion,[1] Jadran Vrabec,[2] and Hans Hasse[1a]

[1] *Laboratory for Engineering Thermodynamics, University of Kaiserslautern, 67663 Kaiserslautern, Germany.*

[2] *Thermodynamics and Energy Technology, University of Paderborn, 33098 Paderborn, Germany.*

(Dated: December 20, 2010)

Density, self-diffusion coefficient and shear viscosity of pure liquid water are predicted for temperatures between 280 and 373 K by molecular dynamics simulation and the Green-Kubo method. Four different rigid non-polarizable water models are assessed: SPC, SPC/E, TIP4P and TIP4P/2005. The pressure dependence of the self-diffusion coefficient and the shear viscosity for pure liquid water is also calculated and the anomalous behavior of these properties is qualitatively well predicted. Furthermore, transport properties as well excess volume and excess enthalpy of aqueous binary mixtures containing methanol or ethanol, based on the SPC/E and TIP4P/2005 water models, are calculated. Under the tested conditions, the TIP4P/2005 model gives the best quantitative and qualitative agreement with experiments for the regarded transport properties. The deviations from experimental data are of 5 to 15% for pure liquid water and 5 to 20% for the water + alcohol mixtures. Moreover, the center of mass power spectrum of water as well as the investigated mixtures are analyzed and the hydrogen-bonding structure is discussed for the different states.

Keywords: Green-Kubo, excess enthalpy, excess volume, TIP4P/2005, TIP4P, SPC/E, water structure, spectral density.

[a] To whom correspondence should be adressed, Email:hans.hasse@mv.uni-kl.de

1 Introduction

The importance of water was recognized already by early civilizations such that it occupied a prominent place in ancient cosmologies and mythologies [1]. Nowadays, it is well known that water plays a key role in biological and chemical processes. Hence, water is one of the most thoroughly investigated substances also due to its unique physical and chemical properties. Mixtures of water and alcohols are also interesting systems, in part due to their complex dynamics resulting from the presence of hydrophobic groups and hydrogen-bonding. These mixtures are also important because of their extensive use as solvents and are thus in the center of long-standing experimental and theoretical investigations.

A thorough knowledge of the transport properties of water and its mixtures with alcohols is particularly significant, since these properties are needed in both natural science and engineering applications. However, they are generally difficult to model accurately, especially with phenomenological approaches. In this context, molecular simulation offers a promising route to predict transport properties and to understand the link between molecular structure and macroscopic behavior.

In the last decades, there has been a quest for a molecular water potential that is capable of reproducing qualitatively and quantitatively all the relevant thermodynamic properties and that is also transferable to aqueous solutions. As early as 1933, Bernal and Fowler [2] proposed the first molecular model of water. Since then, numerous potential models for water have been proposed: rigid, flexible, polarizable, etc. [3]. However, despite the large number of water models in the literature, only a handful is actively being used. The central aim of this work is to reveal the current capabilities and limits of available simple rigid, non-polarizable models for predictions of thermodynamic transport properties of water and its binary mixtures with small alcohols in the liquid phase.

The prediction of transport properties is a challenging test for molecular models. E.g., this task was proposed for mixtures of the type water + short alcohol as a benchmark for water models [4]. In the present work, four commonly used rigid, non-polarizable molecular models from the literature were assessed in this sense: simple point charge (SPC) [5], extended simple point charge (SPC/E) [6], four point transferable intermolecular potential (TIP4P) [7] and a modification thereof (TIP4P/2005) [8]. The two models with the best performance for pure liquid water (SPC/E and TIP4P/2005) were subsequently employed for the simulation of aqueous alcoholic mixtures.

The advantage of all studied molecular models is that they are easy to implement and computationally inexpensive. Most of them have been extensively studied with respect to static and dynamic properties prediction. Vega et al. [9] have recently made a comparison of different rigid, non-polarizable water models for a variety of properties including the self-diffusion coefficient. In general, they found that the TIP4P/2005 water model yields the best results, however, this model have problems predicting properties of the saturated vapor phase [10]. Table 1 shows a comparison of the calculated self-diffusion coefficient of liquid water at around ambient conditions by different authors, e.g., SPC [11–19], SPC/E [6, 13–20], TIP4P [9, 15–17], TIP4P/2005 [9]. Although the simulation results from the literature exhibit some scatter, in most cases, the self-diffusion coefficient of water was significantly overestimated, which will be discussed below in detail. There are also numerous publications on the shear viscosity using the discussed water models, e.g., SPC [12–14,22–24], SPC/E [12–14,23–28], TIP4P [4,28,29] and TIP4P/2005 [28]. However, a direct comparison of the studied models on the basis of literature data is hardly feasible due to the large scatter of the simulation results, which is a consequence of the use of different system size, cut-off radius, electrostatic treatment and simulation methods, cf. Table 2.

In this work, self-diffusion coefficient and shear viscosity were predicted using equilibrium molecular dynamics simulation and the Green-Kubo formalism. A relatively large system size and cut-off radius were chosen to obtain accurate results. Furthermore, both transport properties were predicted in the liquid phase over a wide temperature range.

The potential models for methanol [30] and ethanol [31] used in this work are also rigid, non-polarizable and of united-atom type. Both models were developed in our group and have recently been successfully tested on their ability to predict transport properties of the pure fluids and their binary mixture [32].

Mixtures of water and alcohols show non-idealities for different thermodynamic properties, e.g. self-diffusion coefficient, shear viscosity, excess volume and excess enthalpy. This behavior has been subject of many studies on microscopic and macroscopic properties [33–40]. E.g., the two self-diffusion coefficients of methanol and water in their binary mixture have been predicted using rigid [4, 41–43], flexible [44, 45] and polarizable [46] potentials by molecular simulation. Compared to the aqueous methanol mixture, publications on dynamic properties of aqueous ethanol mixtures by molecular simulation are rather recent [4, 47–50]. On the other hand, many attempts have been made to predict excess volume and excess enthalpy of binary aqueous methanol or ethanol mixtures by molecular simulation [4, 41, 46, 48–54].

The shear viscosity of binary mixtures of water with methanol [4, 55] and ethanol [4] has also been calculated by molecular simulation. However, to our knowledge, the large excess shear viscosity upon mixing was not correctly predicted neither qualitatively nor quantitatively. Most of the published simulation work on aqueous alcoholic mixtures is based on the SPC/E and TIP4P water models and the (UA and AA) OPLS models [56] for the alcohols. In this work, the simulations of aqueous alcoholic mixtures were performed based on the SPC/E and TIP4P/2005 models. There are, to our knowledge, only two previous simulation works on aqueous mixtures where these two models were compared, studying solubility [57] and self-diffusion in the mixture water + formamide [58]. In both works, it was found that the TIP4P/2005 model yields better results. In a recent work, Dopazo-Paz et al. [59] tested the TIP4P, TIP4P/2005 and TIP4P/ice water models for the prediction of first- and second-order excess thermodynamic derivatives for the mixture water + methanol. They found the best agreement with the experimental data for the simulations based on the TIP4P/2005 model.

This paper is organized as follows: first, the molecular models, simulation methodology and technical details are described. Second, the simulation results for density, self-diffusion coefficient and shear viscosity for pure liquid water based on the SPC, SPC/E, TIP4P and TIP4P/2005 models are presented and compared to experimental data. Subsequently, an analysis on differences of the fluid structure due to the water models is made by means of the power spectrum. Simulative predictions for self-diffusion coefficient, shear viscosity, excess enthalpy and excess volume are given for the two binary mixtures: water + methanol and water + ethanol. Both the SPC/E and the TIP4P/2005 models were employed for this task. Additionally, the composition dependence of the spectral density of water and the alcohols in their binary mixtures is investigated. Finally, some conclusions are drawn.

2 Molecular models

Throughout this work, rigid, non-polarizable molecular models of united-atom type were used. The models account for the intermolecular interactions, including hydrogen-bonding, by a set of Lennard-Jones (LJ) sites and point charges which may or may not coincide with the LJ site positions. The potential energy u_{ij} between two molecules i and j can be written as

$$u_{ij}\left(r_{ijab}\right) = \sum_{a=1}^{n}\sum_{b=1}^{m} 4\epsilon_{ab}\left[\left(\frac{\sigma_{ab}}{r_{ijab}}\right)^{12} - \left(\frac{\sigma_{ab}}{r_{ijab}}\right)^{6}\right] + \frac{q_{ia}q_{jb}}{4\pi\varepsilon_0 r_{ijab}}\,, \qquad (1)$$

where a is the site index of molecule i, b the site index of molecule j, while n and m are the numbers of interaction sites of molecules i and j, respectively. r_{ijab} represents the site-site distance between molecules i and j. The LJ size and energy parameters are σ_{ab} and ϵ_{ab}. q_{ia} and q_{jb} are the point charges located at the sites a and b of the molecules i and j, and ε_0 is the permittivity of vacuum.

For water, models with three site positions (SPC and SPC/E) as well as models with four site positions (TIP4P and TIP4P/2005) were used. The molecular models for both methanol and ethanol were taken from prior work [30, 31] as well. The interested reader is referred to the original publications for detailed information about the six molecular pure substance models and their parameters.

To define a molecular model for a binary mixture on the basis of pairwise additive pure substance models, only the unlike interactions have to be specified. In case of polar interaction sites, i.e. point charges here, this can straightforwardly be done using the laws of electrostatics. However, for the unlike LJ parameters there is no physically sound approach [60] and combining rules have to be employed for predictions. Here, the interactions between unlike LJ sites of two molecules were determined by the Lorentz-Berthelot combining rule

$$\sigma_{ab} = \frac{\sigma_{aa} + \sigma_{bb}}{2}\,, \qquad (2)$$

and

$$\epsilon_{ab} = \sqrt{\epsilon_{aa}\epsilon_{bb}}\,. \qquad (3)$$

Thus all mixture data presented below are strictly predictive.

3 Methodology

Transport properties

Throughout, equilibrium molecular dynamics simulation and the Green-Kubo formalism [61, 62] were used to calculate the self-diffusion coefficient and the

shear viscosity. This formalism establishes a direct relationship between a transport coefficient and the time integral of the autocorrelation function of the corresponding microscopic flux in a system in equilibrium.

The Green-Kubo expression for the self-diffusion coefficient D_i is

$$D_i = \frac{1}{3N_i} \int_0^\infty \mathrm{d}t \, \left\langle \mathbf{v}_k(t) \cdot \mathbf{v}_k(0) \right\rangle, \tag{4}$$

where $\mathbf{v}_k(t)$ is the center of mass velocity vector of molecule k at some time t and <...> denotes the ensemble average. Eq. (4) is an average over all N molecules of type i in a simulation, since all contribute to the self-diffusion coefficient.

The shear viscosity η can be related to the time autocorrelation function of the off-diagonal elements of the stress tensor J_p^{xy} [63]

$$\eta = \frac{1}{V k_B T} \int_0^\infty \mathrm{d}t \, \left\langle J_p^{xy}(t) \cdot J_p^{xy}(0) \right\rangle, \tag{5}$$

where V stands for the molar volume, k_B is the Boltzmann constant and T denotes the temperature. Averaging over all three independent elements of the stress tensor, i.e. J_p^{xy}, J_p^{xz} and J_p^{yz}, improves the statistics of the simulation. The component J_p^{xy} of the microscopic stress tensor $\mathbf{J}_p$ is given by [64]

$$J_p^{xy} = \sum_{i=1}^{N} m v_i^x v_i^y - \frac{1}{2} \sum_{i=1}^{N} \sum_{j \neq i}^{N} \sum_{k=1}^{n} \sum_{l=1}^{n} r_{ij}^x \frac{\partial u_{ij}}{\partial r_{kl}^y}. \tag{6}$$

Here, the lower indices l and k count the interaction sites, and the upper indices x and y denote the spatial vector components, e.g. for velocity v_i^x or site-site distance r_{ij}^x. Eqs. (5) and (6) may directly be applied to mixtures.

Excess properties

To determine excess properties, three simulations at a specified pair of temperature and pressure were performed, two for the pure substances and one for the mixture at a specified composition. A binary excess property is then given by

$$y^{\mathrm{E}} = y - x_1 \cdot y_1 - x_2 \cdot y_2, \tag{7}$$

where y^{E} represents the excess volume v^{E} or the excess enthalpy h^{E} here. Enthalpies or volumes of the two pure substances and their binary mixture are denoted by y_1, y_2 and y, respectively.

3.1 Simulation details

Molecular dynamics simulations were performed using the program $ms2$ [65]. These were done in two steps: first, a simulation in the isobaric-isothermal (NpT) ensemble was performed to calculate the density at the desired temperature and pressure. In the second step, a canonic (NVT) ensemble simulation was performed at this temperature and density, to determine the transport properties. Newton's equations of motion were solved using a fifth-order Gear predictor-corrector numerical integrator. The temperature was controlled by velocity scaling. Here, the velocities are scaled such that the actual kinetic energy matches the specified temperature. The scaling is applied equally over all molecular degrees of freedom. In all simulations, the integration time step was 0.98 fs. The simulations were carried out in a cubic box with periodic boundary conditions.

To avoid size and cut-off effects, the influence of the number of particles and the cut-off radius on the predicted self-diffusion coefficient of pure liquid water was studied for two different models, i.e. SPC/E and TIP4P. For small systems containing up to 600 molecules, the self-diffusion coefficient increases significantly with particle number, which agrees with the findings of other authors [15]. For a larger number of particles, the importance of the size effect decreases smoothly as can be seen in Fig. 1. Furthermore, both tested water models show a decrease of the calculated self-diffusion coefficient with increasing cut-off radius, cf. Fig. 1. However, for cut-off radii greater than 15 Å, this dependence is rather weak. Accordingly, given that water shows ordering up to of 14 Å [66], the simulations discussed below were performed using 2048 molecules and the cut-off radius was set to $r_c = 15$ Å. The LJ long range interactions were corrected using angle averaging [67]. Electrostatic long-range corrections were considered by the reaction field technique with conducting boundary conditions ($\epsilon_{RF} = \infty$).

The use of the reaction field for water simulations has recently been challenged by Van der Spoel et al. [16]. They found extreme differences for the self-diffusion coefficient, depending on whether Ewald summation or the reaction field with ($\epsilon_{RF} = 78.5$) was used. However, their results based on the reaction field method deviate strongly from simulation results by other authors and from those of this work as can be seen in Table 1. The present

results agree well with those of Van der Spoel et al. [16] based on particle mesh Ewald (PME).

The simulations in the NpT ensemble were equilibrated over 8×10^4 time steps, followed by a production run over 3×10^5 time steps. When excess properties were evaluated, the equilibration and production runs were longer, 10^5 and 5×10^5 time steps, respectively.

In the NVT ensemble, the simulations were equilibrated over 10^5 time steps, followed by production runs of 1 to 2.5×10^6 time steps. The self-diffusion coefficient and the shear viscosity were calculated by Eqs. (4) to (6) with up to 1.4×10^3 independent time origins of the autocorrelation functions. The sampling length of the autocorrelation functions varied between 9 and 14 ps. The separation between the time origins was chosen such that all autocorrelation functions have decayed at least to $1/e$ of their normalized value to achieve their time independence [68]. The uncertainties of the predicted values were estimated using a block averaging method [69].

4 Simulation results of pure water

4.1 Density

The calculated liquid water density at ambient pressure is shown for a range of 100 K around ambient temperature in Fig. 2 for the four tested models together with a correlation of experimental data [70]. Numerical simulation results are given in the Table 1 of the supplementary material. In the studied temperature range, the best results were obtained with TIP4P/2005. This finding is not surprising, since the TIP4P/2005 model was parameterized to reproduce the water density maximum [8]. Although the SPC/E and TIP4P models perform fairly well at ambient temperature, the predicted water density deviates strongly from experimental values for temperatures above 320 K. The performance of the SPC model is not good in the whole regarded temperature range. Likewise, it has been shown [9] that the TIP4P/2005 model performs also better than other commonly used rigid, non-polarizable models not considered here, e.g. TIP4P/Ew, TIP3P and TIP5P.

4.2 Self-diffusion coefficient

The self-diffusion coefficient of pure liquid water was predicted at 0.1 MPa in the temperature range from 280 to 360 K for all four water models consid-

ered here. Present numerical data are given in the supplementary material (Table 1). The obtained values for the self-diffusion coefficient are in good agreement with the results published by other authors, cf. Table 1. Fig. 3 shows experimental and predicted values for the self-diffusion coefficient as a function of temperature. The statistical error of the simulation data is estimated to be in the order of 1%. In the studied temperature range, the mobility of the SPC, SPC/E and TIP4P molecular models is higher than that of real water molecules, hence, the self-diffusion coefficient is overestimated. On the other hand, the predictions on the basis of the TIP4P/2005 model are in very good agreement with the experimental data. At temperatures above 330 K, a tendency to underestimate the self-diffusion coefficient could be inferred, however, care should be taken due to the large scatter of the experimental data.

Since the results at ambient pressure on the basis of the TIP4P/2005 model are very satisfactory, additional calculations for pressures up to 300 MPa were performed for that model. The simulation results are listed in the supplementary material (Table 2). As an example, the results for 200 MPa are plotted in Fig. 4 together with experimental data. In general, a very good agreement between simulation results and experimental data was found for the studied temperature and pressure range. In contrast to most molecular liquids, the self-diffusion coefficient of water increases with pressure at temperatures below 300 K. This anomalous behavior was qualitatively predicted here, cf. Fig. 5. Pi et al. [80] also observed that behavior for TIP4P/2005 at pressures up to 100 MPa and temperatures below 280 K. However, there is an overestimation of the increase of the self-diffusion coefficient at 273.15 K, and the pressure at which it starts to decrease is higher than that observed experimentally. These results suggest a less developed structure in the TIP4P/2005 fluid close to the triple point, which allows more hydrogen-bond breaking due to pressure than in case of real water. It should be noted that this anomaly was also predicted by other authors using the SPC/E [81–84] and TIP4P [85] models. However, the reported values [81–84] are only in qualitative agreement with experimental data, as the predicted increase of the self-diffusion coefficient is mostly significantly lower.

4.3 Shear viscosity

The shear viscosity of pure liquid water was predicted at 0.1 MPa in the temperature range from 275 to 360 K using the four studied water models. Numerical data are given in the supplementary material (Table 1). Within their statistical uncertainties (10 to 17%), the present simulation results at

298.15 K are in agreement with the shear viscosity values published by other authors at similar temperatures using NEMD and EMD methods, cf. Table 2.

In Fig. 6, the predicted shear viscosity is shown a function of temperature and compared to a correlation of experimental data [86]. As found by other authors, cf. Table 2, the shear viscosity of water is generally underestimated by the SPC, SPC/E and TIP4P models. This is consistent with the overestimation of the self-diffusion coefficient, as indicated by the Stokes-Einstein relationship. Accordingly, the shear viscosity obtained with the TIP4P/2005 model shows the best agreement with the experimental data.

As for the self-diffusion coefficient, the shear viscosity of pure liquid water was predicted for pressures up to 300 MPa using the TIP4P/2005 model. The results are given in the supplementary material (Table 2). In general, the present shear viscosity values are in very good agreement with the experiment. Exemplarily, Fig. 7 shows the calculated shear viscosity at 200 MPa compared to a correlation of experimental data [86]. The anomalous decrease of the shear viscosity with pressure at temperatures below 300 K can be inferred from the present results, unfortunately, due to the high uncertainties of the simulation results, a sound conclusion cannot be made.

4.4 Power spectrum

Autocorrelation functions provide an interesting insight into the liquid state. They decay fast and generally show short memory effects due to the strong interaction of individual molecules with their nearest neighbors. In this work, the velocity autocorrelation function (VACF) of water was calculated to determine the self-diffusion coefficient. The VACF can be analyzed more deeply when the Fourier transform of the VACF is regarded. The resulting power spectrum provide information on the frequency of the bands in the IR spectrum of the liquid. Thereby, some qualitative characteristics of the IR bands for model fluids can be predicted. Power spectra are commonly studied when flexible models are used, but also provide interesting information for the rigid models studied here. The power spectrum $S(\omega)$ of a given autocorrelation function $C(t)$ is given by [87]

$$S(\omega) = \int_0^\infty \mathrm{d}t \; C(t) \cdot \cos(\omega t). \tag{8}$$

The center of mass spectral densities at low frequencies obtained thereby are related to the translational motions of the molecules. Fig. 8 shows the nor-

malized spectral densities at 280 K and 0.1 MPa for the SPC, SPC/E, TIP4P and TIP4P/2005 models. All spectra show a maximum close to 50 cm^{-1} (peak I) and a second peak (II) at around 250 cm^{-1}. These peaks have been associated with the IR bands near 60 cm^{-1} and 170 cm^{-1} observed in Raman measurements [88, 89]. Peak I has been attributed to the bending motion of the O···O···O angle [88], but also to the backscattering or vibration of water molecules inside the cage formed by their nearest neighbors [90]. Peak II is believed to be related to the restricted translation of two hydrogen-bonded molecules against each other along the O−H···O direction [88]. Martí et al. [90] have shown that this peak of the spectral density is less pronounced when the number of hydrogen-bonds decreases. This suggests that the peak at low frequency characterizes the strength of the hydrogen-bonded structure of the cage of neighbors, while the peak at high frequencies indicates the strength of the hydrogen-bond.

The intensity and to a lesser extent the position of the peaks in the power spectrum varies for the different water models. Peak I is the highest for the TIP4P/2005 model, followed by the SPC/E and TIP4P models. This suggests the presence of a more stable structure in TIP4P/2005 water, which could explain the lower and more appropriate values of the self-diffusion coefficient. For the three site water models, peak II is less pronounced and slightly shifted to higher frequencies. TIP4P/2005 water also shows the highest peak II. Accordingly, it could be inferred that TIP4P/2005 water exhibits the strongest hydrogen-bonding network among the studied models.

The intensity of peak II decreases when the temperature increases, cf. Fig. 9. This change has been associated with the break down of the hydrogen-bonded network [88]. Fig. 10 shows the change of the power spectrum of TIP4P/2005 water with pressure at 280 K. The magnitude of peak II decreases with increasing pressure. This implies a distortion of the hydrogen-bonds with pressure, which is considered to be the main reason of the enhancement of the self-diffusion coefficient with increasing pressure [79,91,92]. At temperatures above around 310 K, the self-diffusion anomaly can not be observed anymore and peak II is more pronounced and somewhat shifted to higher frequencies, cf. inset in Fig. 10. These results suggest an increase in the hydrogen-bonding strength due to compression.

5 Simulation results of binary aqueous mixtures

5.1 Water + Methanol

Self-diffusion coefficient

Self-diffusion coefficients of water and methanol in their binary mixture were predicted on the basis of the methanol model developed in prior work of our group [30] as well as the SPC/E and TIP4P/2005 water models at ambient conditions for the entire composition range. Numerical simulation results are presented in Table 3 of the supplementary material. The estimated statistical uncertainty of the simulation data is between 1 and 2%. Fig. 11 shows the comparison between present simulation results on the basis of the TIP4P/2005 model and the experimental values of the self-diffusion coefficients of water and methanol at 278.15 and 298.15 K. Unfortunately, the reported experimental data are somewhat contradictory, especially for water. Considering these uncertainties, a good agreement between the predicted self-diffusion coefficients of water and methanol with the experimental data was found, i.e. the largest deviations are approximately 14% at the minimum of the self-diffusion coefficient. Furthermore, the composition dependence of this property is correctly predicted for both components. The self-diffusion coefficients on the basis of the SPC/E model (not shown graphically) are around 5 to 25% higher than the values obtained for the TIP4P/2005 model and hence, further off the experimental data.

In comparison to other rigid water models, the combination of the TIP4P/2005 model and the methanol model by Schnabel et al. [30] show the best performance for predicting of the self-diffusion coefficients of both components in their mixture. For instance, both self-diffusion coefficients were overestimated by 30 to 70% using the TIP4P model for water and the AA−OPLS model for methanol by Wensink et al. [4]. The predictions of Weerasinghe and Smith [41], using the SPC/E model and a Kirkwood-Buff derived force field for methanol, are significantly too high at low methanol mole fractions and the self-diffusion coefficient minima for both water and methanol are shifted to $x_{\mathrm{MeOH}} = 0.8$ mol/mol. Ferrario et al. [42] used the TIP4P water model together with their own methanol model [94] to obtain the self-diffusion coefficients. Their pioneering simulation results are in relatively good agreement with the experiment, but show a large scatter and high statistical uncertainties. Zhong et al. [46] used rigid, polarizable force fields and underestimated

the self-diffusion coefficient of both components by about 20%. The present results are comparable in accuracy to the predictions by Pálinkás et al. [44] and Hawlicka et al. [45] based on more complex flexible models.

Shear viscosity

Table 3 of the supplementary material lists the numerical simulation results for the mixture methanol + water at ambient conditions in the entire composition range as obtained in the present work with the SPC/E and TIP4P/2005 water models and the methanol model by Schnabel et al. The estimated simulation uncertainty is on average 12%. Fig. 12 shows the predicted shear viscosity at 278.15 and 298.15 K for the TIP4P/2005 model together with experimental data. The non-ideality of the shear viscosity at low methanol mole fractions is qualitatively predicted with both tested water models (SPC/E results are not shown graphically), however, the predictions based on the TIP4P/2005 model are also quantitatively correct. Simulation results based on the TIP4P/2005 model deviate from the experiment on average by 4% at 298.15 K and by 12% at 278.15 K. The maximum deviation at 278.15 K is about −14% and occurs around the shear viscosity maximum, which is enhanced when the temperature is low.

There are only a few works on the shear viscosity of this mixture based on other models. E.g., at ambient conditions, the simulation results of Wheeler et al. [55], using the SPC/E model for water and the methanol model by van Leeuwen and Smit [98], underpredicted the shear viscosity by 15% on average, with deviations of up to −25% from experimental values. The results by Wensink et al. [4], using the TIP4P model for water and the AA−OPLS model for methanol, deviate between −25 and −50% from the experiment.

Power spectrum

To obtain an insight on the influence of the neighborhood on the average individual molecular motion, the center of mass spectral density of both components in their mixture was analyzed. Fig. 13 shows the normalized power spectrum of pure liquid methanol and that of methanol in aqueous liquid mixtures with different compositions. The power spectrum of pure methanol is similar to that of pure water, it exhibits a maximum close to 50 cm^{-1} (peak I) and a shoulder at around 150 cm^{-1} (peak II). Analogously, peak I can be assigned to the motion of the particles inside the cage formed by their neighbors. However, in contrast to water, this band is not found

experimentally [87]. Peak II can be related to the presence and the strength of hydrogen-bonding. Upon addition of water, peak II of the methanol spectral density gradually disappears, suggesting the break down of the hydrogen-bonded methanol chains, which is in agreement with experimental Raman observations [99] and other MD studies [39, 42, 44]. At the same time, peak I grows and broadens, which could be a consequence of an increasing number of neighboring water molecules around the methanol molecules. At $x_{\mathrm{MeOH}} \simeq 0.3$ mol/mol, only peak I can be observed in the power spectrum and it decreases in magnitude upon further increase of water concentration. This suggests the presence of a very stable structure around methanol molecules, which coincides with the self-diffusion coefficient minimum, cf. Fig. 13. For higher water mole fractions, peak I becomes gradually shorter and narrower, reflecting a weakening of the cage structure. Moreover, a shoulder at around 250 cm^{-1} (peak III) appears, which could be related to the presence of strong water-methanol hydrogen-bonding.

The normalized spectral density of water in the liquid mixture water + methanol is shown in Fig. 14 for selected compositions. As discussed above, the pure water spectrum shows two well defined peaks. When methanol is added up to a mole fraction of $x_{\mathrm{MeOH}} \simeq 0.3$ mol/mol, both peaks increase in magnitude, which suggests the presence of more stable water structures than in pure water. The origin and nature of this enhanced water structure has been subject of many experimental and theoretical studies, e.g. [39, 44, 100–102]. Since the shape of peak I remains almost constant, no significant changes in composition or in the structure of the cage of neighbors are expected. Hence, the present results are consistent with the presence of water clusters with a further stabilization of the tetrahedral cage structure.

When the methanol concentration is increased to the self-diffusion minimum mole fraction at $x_{\mathrm{MeOH}} \simeq 0.4$ mol/mol, peak I remains unchanged, while peak II reaches a maximum. Hence, it could be inferred that the water hydrogen-bonded structure of the cage is strengthened, while the interactions with methanol molecules hardly change. This is consistent with the presence of a hydration structure around the alcohol molecules [40]. For higher methanol mole fractions, the main feature of the power spectrum is the progressive appearance of a shoulder at around 170 cm^{-1} (peak III), which could be related to the presence of water-methanol hydrogen-bonds. Moreover, peak I has a lower magnitude and is shifted to lower frequencies, suggesting a change in structure and in composition of the cage of neighbors.

Excess volume and excess enthalpy

Excess volume and excess enthalpy are basic mixing properties. In case of water + methanol, the non-ideal mixing effects are very strong. Table 4 of the supplementary material contains the present numerical simulation results from the TIP4P/2005 water model at ambient conditions. They are compared in Figs. 15 and 16 to experimental data, present results based on the SPC/E model and those based on other models reported in the literature.

The predicted excess volume from the TIP4P/2005 model, cf. Fig. 15, agrees better with the experiment than that from the SPC/E model. In general, there is a fair agreement with the experiment, however, the simulation data yield less pronounced (negative) excess volumes at equimolar composition, where the influence of mixing is strongest. Here, the excess volume, predicted on the basis of the TIP4P/2005 model, is off by about 20%. The present results are unexpectedly similar to those based on the TIP4P model for water and the UA−OPLS model for methanol by González-Salgado and Nezbeda [51], who also employed different mixing rules. The results of Freitas [54], using the same models and mixing rules as [51], are in somewhat better agreement with the experimental data for $x_{\mathrm{MeOH}} < 0.5$ mol/mol. Similar results with a slight shift of the excess volume minimum towards higher methanol mole fractions were obtained by Wensink et al. [4] using the TIP4P model for water and the AA−OPLS model for methanol. On the other hand, the excess volume was predicted with a very good accuracy from a Kirkwood-Buff derived force field for methanol and the SPC/E model for water by Weerasinghe and Smith [41].

In Figure 16, present results for the excess enthalpy on the basis of the SPC/E and TIP4P/2005 models are shown together with simulation data from the literature and experimental data. The agreement of both present predictions is poor for $x_{\mathrm{MeOH}} < 0.8$ mol/mol. The results for the TIP4P/2005 model are just slightly better than those found in the literature for the TIP4P water model together with the UA−OPLS [51] and the AA−OPLS [41] models for methanol. The results based on the same molecular models (TIP4P and UA−OPLS) by Koh et al. [52] and Freitas [54] are mostly in better agreement with the experiment, but their data strongly scatter and have large uncertainties. It has been argued that the poor results obtained with non-polarizable models are because of the presence of significant polarization effects [41]. However, the values of the excess enthalpy reported by Zhong et al. [46] and Yu et al. [53], using polarizable molecular models, are not significantly better.

After submission of the reviewd version of this paper, we bacame aware of

the work of Perera et al. [116] on the prediction of excess enthalpy and volume of the mixture water + methanol by molecular simulation on the basis of the SPC/E model for water and the OPLS model for methanol. Their results are similar to present simulation data using the SPC/E model of water.

5.2 Water + Ethanol

Self-diffusion coefficient

The self-diffusion coefficients of water and ethanol were predicted in their binary mixture on the basis of the SPC/E and TIP4P/2005 water models and the ethanol model by Schnabel et al. [31] at ambient conditions for the entire composition range. Numerical results with an estimated statistical uncertainty of 1 to 2% are listed in Table 5 of the supplementary material. Fig. 17 shows the predicted self-diffusion coefficients of water and ethanol in their mixture at 278.15 and 298.15 K on the basis of the TIP4P/2005 model compared to experimental values as far as available. The agreement between the predicted self-diffusion coefficients and the experimental data is good for both components. The present data mostly slightly underestimate the self-diffusion coefficients, especially in the ethanol-rich region, where the deviations from experimental values are up to 9% for ethanol and up to 13% for water. The composition of the ethanol self-diffusion coefficient minimum, predicted to be $x_{\mathrm{EtOH}} \simeq 0.25$ mol/mol, is in good agreement with the experiment ($x_{\mathrm{EtOH}} \simeq 0.2$ mol/mol [40]). Similar findings hold for the self-diffusion coefficient of water, for which the minimum is shifted towards higher ethanol concentrations. On the other hand, the self-diffusion coefficients obtained on the basis of the SPC/E model are mostly higher than the experimental values (up to 35%, not shown graphically), especially in the water-rich composition range. Moreover, the self-diffusion minima of both ethanol and water are strongly shifted towards the ethanol-rich composition range.

The predictions obtained in this work on the basis of the TIP4P/2005 model are in better agreement with the available experimental data than those published for other molecular models. E.g., the self-diffusion coefficients of water and ethanol have been significantly overestimated over the whole composition range using the TIP4P model for water and the AA−OPLS model for ethanol [4]. The predictions by Müller-Plathe [49] and those by Zhang et al. [47], using the same SPC water model but different rigid, all atom models for ethanol, are up to 50% higher than the experimental values and the self-diffusion minima are shifted towards higher ethanol concentrations. Even though the compositions of the self-diffusion coefficient minima

were correctly predicted using polarizable models in the work of Noskov et al. [48], their absolute values are almost throughout too low with deviations of up to −40%.

Shear viscosity

The present predicted shear viscosity data for the binary mixture water + ethanol for the SPC/E and TIP4P/2005 models at ambient conditions in the entire composition range are listed in Table 5 of the supplementary material. The estimated statistical uncertainty is on average 13%. Simulation data are compared to experimental data on the basis of the TIP4P/2005 model in Fig. 18. In general, the shear viscosity agrees well with the experiment for both models (SPC/E not shown graphically). Nevertheless, the data obtained using the TIP4P/2005 model are more accurate, despite an underestimation of the shear viscosity maximum of about −15%. For lower temperatures, where the non-ideality of the mixture is enhanced, the predictions are still good in absolute terms as can be seen in Fig. 18. However, it should be noted that the statistical accuracy of the predictions is somewhat lower.

To our knowledge, there is only one previous prediction of the shear viscosity of this mixture by molecular simulation. Wensink et al. [4] used the TIP4P model for water and the AA−OPLS model for ethanol and found larger deviations from the experimental data.

Power spectrum

The center of mass power spectra of the mixture water + ethanol were analyzed at ambient conditions for different compositions. The spectral density of pure ethanol shows a low frequency band centered at around 30 cm^{-1} (peak I), which similarly to peak I of the power spectrum of pure water and pure methanol, can be related to the vibration of molecules inside their cage of neighbors, cf. Fig. 19. The weakly pronounced shoulder at frequencies between 200 and 250 cm^{-1} (peak II) was associated with the degree of hydrogen-bonding by Saiz et al. [110]. In the mixture water + ethanol, the magnitude of peak I in the ethanol spectrum increases, hardly changing its shape, up to a mole fraction of $x_{\mathrm{EtOH}} \simeq 0.5$ mol/mol, while peak II slightly shifts to higher frequencies. These results suggest an increase in the self-association strength of ethanol molecules, which is consistent with the decrease of the self-diffusion coefficient and the presence of the critical percolation point of water at x_{EtOH} slightly below 0.5 mol/mol [47]. Upon further

increase of the water content, i.e. $x_{\mathrm{EtOH}} = 0.5$ to 0.25 mol/mol, the shape of peak I changes significantly, it shifts to higher frequencies, broadens and its magnitude increases slowly to reach a maximum. This peak magnitude maximum corresponds to the self-diffusion coefficient minimum, cf. Fig. 19, and can be related to the formation of a stable cage structure, where water molecules are gradually included. For $x_{\mathrm{EtOH}} < 0.25$ mol/mol, the right-shift and the change of the shape of peaks I and II become more apparent. This implies a qualitative change of the ethanol neighbors, associated with a decrease of the strength of the cage structure.

Fig. 20 shows the normalized spectral density of water in its mixture with ethanol at different compositions. Similarly to the power spectrum of water in its mixture with methanol, the two characteristic water peaks increase with increasing ethanol mole fraction, keeping their shape up to a mole fraction of $x_{\mathrm{EtOH}} = 0.4$ mol/mol. These results indicate the presence of water clusters with a strengthened hydrogen-bond network, as suggested by nuclear magnetic resonance experiments [111] and molecular dynamics studies [47]. By increasing the ethanol content, i.e. $x_{\mathrm{EtOH}} > 0.5$ mol/mol, peak I gradually flattens while peak II increases in magnitude. This suggests the distortion of the structure of the cage of neighbors, caused by the presence of ethanol molecules, but also a modification in the hydrogen-bonding characteristics. Hence, it can be deduced that the slow change of the self-diffusion coefficient of water in this composition range is a result of a trade-off between the freedom of movement due to the distortion of the cage structure and the formation or the strengthening of hydrogen-bonds. Note that a higher peak II, being shifted to lower frequencies, could be an indication for the formation of strong water-ethanol hydrogen-bonds, being in agreement to chemical shift studies [111, 112] and the increase in the total number of hydrogen-bonds as supported by excess entropy measurements [113].

Excess volume and excess enthalpy

The volume and enthalpy as well as their excess values for the mixture water + ethanol are listed in Table 6 of the supplementary material. The simulation results based on the TIP4P/2005 and SPC/E models are compared to experimental data at ambient conditions, cf. Figs. 21 and 22.

The predicted excess volume based on the TIP4P/2005 model, cf. Fig. 21, agrees better with the experiment in all cases than that based on the SPC/E model. A qualitative agreement with the experiment was achieved with the TIP4P/2005 model. However, there is a tendency of the simulation data

towards a less negative excess volume, especially near equimolar composition, where the deviation is up to 20%. As can be seen in Fig. 21, the present results are slightly more accurate than the ones for the TIP4P model for water in combination with the AA−OPLS model for ethanol as reported by Wensink et al. [4].

Fig. 22 shows the predicted excess enthalpy on the basis of the SPC/E and TIP4P/2005 models in comparison to experimental data and predictions by other authors. The results based on the TIP4P/2005 model agree well with the experiment, despite a small shift in the position of the minimum. Nonetheless, the present results are valuable since rigid, non-polarizable models were used. The predictions of the excess enthalpy found in the literature for other molecular models are rather poor [4, 49], with the exception of the qualitatively correct predictions of Zhang et al. [50]. They used the TIP4P model for water and a modification of the rigid ethanol model by van Leeuwen [115], obtaining similar results to those of this work for the SPC/E model, which are too low in absolute terms.

6 Conclusion

In this work the current capabilities of molecular modelling and simulation for the prediction of transport properties of pure liquid water and its mixtures with methanol and ethanol using classical rigid, non-polarizable models are studied. Furthermore, some information on the hydrogen-bonding structure in these fluids was obtained through the center of mass power spectra. It was shown that transport properties can be predicted on the basis of little sophisticated molecular models with good accuracy, when the TIP4P/2005 water model is used together with the methanol and ethanol models by Schnabel et al. [30, 31]. Hence, the use of flexible or polarizable models is not necessarily required. A careful parameterization of the pure substance molecular models and the use of adequate simulation methods are of greater importance. However, the poor prediction of the excess enthalpy of the mixture water + methanol clearly shows that there are still limitations to be overcome.

Although most of the molecular dynamics simulation work in the literature on water or aqueous mixtures is based on the SPC/E model, the present results show, in agreement with other recent studies, the superiority of the TIP4P/2005 model for the prediction of transport and excess properties. Furthermore, present analysis suggest that TIP4P/2005 water exhibits the strongest hydrogen-bonding network among the regarded models. Therefore, the TIP4P/2005 model should be preferred in the liquid state, not only for

the present applications, but also for the study of dynamic processes such as protein folding, where the hydrogen-bonding structure of water plays a significant role and computationally inexpensive water models are needed. Nevertheless, the TIP4P/2005 model should be used carefully, since it fails to describe the properties of the saturated vapor phase.

Acknowledgments

The simulations were performed on the national super computer NEC SX-8 at the High Performance Computing Center Stuttgart (HLRS) and on the HP X6000 super computer at the Steinbuch Center for Computing, Karlsruhe under the grant LAMO. The presented research was conducted under the auspices of the Boltzmann-Zuse Society of Computational Molecular Engineering (BZS).

References

[1] P. Kramer and J. Boyer, *Water Relations of Plants and Soils* (Academic Press, San Diego, 1995) p.16.

[2] J. D. Bernal and R. H. Fowler, J. Chem. Phys. **1**, 515 (1933).

[3] B. Guillot, J. Mol. Liq. **101**, 219 (2002).

[4] E. J. W. Wensink, C. Hoffmann, P. J. van Maaren and D. van der Spoel, J. Chem. Phys. **119**, 7308 (2003).

[5] H. J. C. Berendsen, J. P. M. Postma, W. F. van Gusteren and J. Hermans, *Intermolecular Forces*, edited by B. Pullman (Reidel, Dordrecht, 1981) p.331.

[6] H. J. C. Berendsen, J. R. Grigera and T. P. Straatsma, J. Phys. Chem. **91**, 6269 (1987).

[7] W. L. Jorgensen, J. Chandrasekhar, J. D. Madura, R. W. Impey and M. L. Klein, J. Chem. Phys. **79**, 926 (1983).

[8] J. L. F. Abascal and C. Vega, J. Chem. Phys. **123**, 234505 (2005).

[9] C. Vega, J. L. F Abascal, M. M. Conde and J. L. Aragones, Faraday Discuss. **141**, 251 (2009).

[10] C. Vega, J. L. F Abascal and I. Nezbeda, J. Chem. Phys. **125**, 034503 (2006).

[11] M. Prevost, D. van Belle, G. Lippens and S. Wodak, Mol. Phys. **71**, 587 (1990).

[12] P. E. Smith and W. F. Gunsteren, Chem. Phys. Lett. **215**, 315 (1993).

[13] Y. Wu, H. L. Tepper and G. A. Voth, J. Chem. Phys. **124**, 024503 (2006).

[14] A. Glättli, X. Daura and W. F. van Gunsteren, J. Chem. Phys. **116**, 9811 (2002).

[15] D. van der Spoel, P. J. van Maaren and J. C. Berendsen, J. Chem. Phys. **108**, 10220 (1998).

[16] D. van der Spoel and P. J. van Maaren, J. Chem. Theory Comput. **2**, 1 (2006).

[17] K. Watanabe and M. L. Klein, Chem. Phys. **131**, 157 (1989).

[18] P. Mark, and L. Nilsson, J. Phys. Chem. A **105**, 9954 (2001).

[19] M. W. Mahoney and W. L. Jorgensen, J. Chem. Phys. **114**, 363 (2001).

[20] A. Chandra and T. Ichiye, J. Chem. Phys. **111**, 2701 (1999).

[21] H. W. Horn, W. C. Swope, J. W. Pitera, J. D. Madura, T. J. Dick, G. L. Hura and T. Head-Gordon, J. Chem. Phys. **120**, 9665 (2004).

[22] P. T. Cummings and T. L. Varner, J. Chem. Phys. **89**, 6391 (1988).

[23] B. Hess, J. Chem. Phys. **116**, 209 (2002).

[24] T. Chen, B. Smit and A.T. Bell, J. Chem. Phys. **131**, 246101 (2009).

[25] S. Balasubramanian, C. J. van Mundy and M. L. Klein, J. Chem. Phys. **105**, 11190 (1996).

[26] J. T. Slusher, Mol. Phys. **98**, 287 (2000).

[27] G. J. Guo and Y. G. Zhang, Mol. Phys. **99**, 283 (2001).

[28] M. A. González and J. L. F. Abascal, J. Chem. Phys. **132**, 096101 (2010).

[29] D. Bertolini and A. Tani, Phys. Rev. E **52**, 1699 (1995).

[30] T. Schnabel, A. Srivastava, J. Vrabec and H. Hasse, J. Phys. Chem. B **111**, 9871 (2007).

[31] T. Schnabel, J. Vrabec and H. Hasse, Fluid Phase Equil. **233**, 134 (2005).

[32] G. Guevara-Carrion, C. Nieto-Draghi, J. Vrabec and H. Hasse, J. Phys. Chem. B **112**, 16664 (2008).

[33] L. Dougan, R. Hargreaves, S. P. Bates, J. L. Finney, V. Réat, A. K. Soper and J. Crain, J. Chem. Phys. **122**, 174514 (2005).

[34] C. Nieto-Draghi, R. Hargreaves and S. P. Bates, J. Phys.: Condens. Matter **17**, S3265 (2005).

[35] T. S. van Erp and E. J. Meijer, J. Chem. Phys. **118**, 8831 (2003).

[36] T. S. van Erp and E. J. Meijer, Chem. Phys. Lett. **333**, 290 (2001).

[37] J.T. Slusher, Fluid Phase Equil. **154**, 181 (1999).

[38] B. Kvamme, Fluid Phase Equil. **131**, 1 (1997).

[39] A. Laaksonen, P. G. Kusalik and I. M. Svishchev, J. Phys. Chem. **101**, 5910 (1997).

[40] W. S. Price, H. Ide and Y. Arata, J. Phys. Chem. A **107**, 4784 (2003).

[41] S. Weerasinghe and P. E. Smith, J. Phys. Chem. B **109**, 15080 (2005).

[42] M. Ferrario, M. Haughney, I. R. McDonald and M. L. Klein, J. Chem. Phys. **93**, 5156 (1990).

[43] I. M. J. J. van de Ven-Lucassen, T. J. H. Vlugt, A. J. J. van der Zanden and P. J. A. M. Merkhof, Mol. Sim. **23**, 79 (1999).

[44] G. Pálinkás, I. Bakó and K. Heinzinger, Mol. Phys. **73**, 897 (1991).

[45] E. Hawlicka and D. Swiatla-Wojcik, Phys. Chem. Chem. Phys. **2**, 3175 (2000).

[46] Y. Zhong, G. L. Warren and S. Patel, J. Comput. Chem. **29**, 1142 (2008).

[47] L. Zhang, Q. Wang, and Y. C. Liu, J. Chem. Phys. **125**, 104502 (2006).

[48] S. Y. Noskov, G. Lamoureux and B. Roux, J. Phys. Chem. B **109**, 6705 (2005).

[49] F. Müller-Plathe, Mol. Simul. **18**, 133 (1996).

[50] C. Zhang, and X. Yang, Fluid Phase Equil. **231**, 1 (2005).

[51] D. González-Salgado and I. Nezbeda, Fluid Phase Equil. **240**, 161 (2006).

[52] C. Koh, H. Tanaka, J. M. Walsh, K. E. Gubbins and J. A. Zollweg, Fluid Phase Equil. **83**, 51 (1993).

[53] H. Yu, D. P. Geerke, H. Liu and W. F. van Gunsteren, J. Comput. Chem. **27**, 1494 (2006).

[54] L. C. Gomide Freitas, J. Mol. Struct. **282**, 151 (1993).

[55] D. R. Wheeler and R. L. Rowley, Mol. Phys. **94**, 555 (1998).

[56] W. L. Jorgensen, J. Phys. Chem. **90**, 1276 (1986).

[57] P. J. Dyer, H. Docherty and P. T. Cummings, J. Chem. Phys. **129**, 024508 (2008).

[58] M. D. Elola and M. L. Branka, J. Chem. Phys. **125**, 184506 (2006).

[59] Y. Dopazo-Paz, P. Gómez-Álvarez and D. González-Salgado, Collect. Czech. Chem. Commun. **75**, 617 (2010).

[60] A. J. Haslam, A. Galindo and G. Jackson, Fluid Phase Equil. **266**, 105 (2008).

[61] M. S. Green, J. Chem. Phys. **22**, 398 (1954).

[62] R. Kubo, J. Phys. Soc. Jpn. **12**, 570 (1957).

[63] K. E. Gubbins, *Statistical Mechanics,* Vol. 1 (The Chemical Society Burlington house, London, 1972).

[64] C. Hoheisel, Phys. Rep. **245**, 111 (1994).

[65] S. Deublein, B. Eckl, J. Stoll, S. V. Lishchuk, G. Guevara-Carrion, C. W. Glass, T. Merker, M. Bernreuther, J. Vrabec and H. Hasse, "ms2: A Molecular Simulation Tool for Thermodynamic Properties", Comput. Phys. Commun. (submitted).

[66] C. Chipot, C. Milot, B. Migret and P. A. Kollman, J. Chem. Phys. **101**, 7953 (1994).

[67] R. Lustig, Mol. Phys. **65**, 175 (1988).

[68] M. Schoen and C. Hoheisel, Mol. Phys. **52**, 33 (1984).

[69] M. P. Allen and D. J. Tidesley, *Computer Simulation of Liquids,* 2nd ed., (Clarendon, Oxford,1987).

[70] W. Wagner and A. Pruss, J. Phys. Chem. Ref. Data **31**, 387 (2002).

[71] F. A. L. Dullien, AIChE J. **18**, 62 (1972).

[72] K. T. Gillen, D. C. Douglass and M. J. R. Hoch, J. Chem. Phys. **57**, 5117 (1972).

[73] R. Mills, J. Phys. Chem. **77**, 685 (1973).

[74] K. R. Harris and L. A. Woolf, J. Chem. Soc., Faraday Trans. 1 **76**, 377 (1980).

[75] A. J. Easteal, W. E. Price and L. A. Woolf, J. Chem. Soc., Faraday Trans. 1 **85**, 1091 (1989).

[76] M. Holz, S. R. Heil and A. Sacco, Phys. Chem. Chem. Phys. **2**, 4740 (2000).

[77] K. Yoshida, C. Wakai, N. Matubayasi and M. Nakahara, J. Chem. Phys. **123**, 164506 (2005).

[78] K. R. Harris and P. J. Newitt, J. Chem. Eng. Data **42**, 346 (1997).

[79] K. Krynicki, C. D. Green and D.W. Sawyer, Faraday Discuss. Chem. Soc. **66**, 199 (1978).

[80] H. L. Pi, J. L. Aragones, C. Vega, E. G. Noya, J. L. F. Abascal, M. Gonzalez and C. McBride, Mol. Phys. **107**, 365 (2009).

[81] K. Bagchi, S. Balasubramanian and M. L. Klein, J. Chem. Phys. **107**, 8561 (1997).

[82] F. W. Starr, S. Harrington, F. Sciortino and H. E. Stanley, Phys. Rev. Lett. **82**, 3629 (1999).

[83] A. Scala, F. W. Starr, W. La Nave, F. Sciortino and H. E. Stanley, Nature **406**, 166 (2000).

[84] P. A. Netz, F. Starr, M. C. Barbosa and H. E. Stanley, J. Mol. Liq. **101**, 159 (2002).

[85] R. Reddy and M. Berkowitz, J. Chem. Phys. **87**, 6682 (1987).

[86] J. Kestin, J. V. Sengers, B. Kamgar-Parsi, and J. M. H. Levelt Sengers, J. Phys. Chem. Ref. Data **13**, 175 (1984).

[87] J. Martí, J. A. Padró and E. Guàrdia, J. Mol. Liq. **64**, 1 (1995).

[88] G. E. Walrafen, M. R. Fisher, M. S. Hokmadabi and W. -H. Yang, J. Chem. Phys. **85**, 6970 (1986).

[89] P. A. Madden and R. W. Impey, Chem. Phys. Lett. **123**, 502 (1986).

[90] J. Martí, J. A. Padró and E. Guàrdia, J. Chem. Phys. **105**, 639 (1996).

[91] F. X. Prielmeier, E. W. Lang, R. J. Speedy, J. and H. -D. Lüdemann, Phys. Rev. Lett. **59**, 1128 (1987).

[92] J. R. Errington and P. G. Debenedetti, Nature **409**, 318 (2001).

[93] Z. J. Derlacki, A. J. Easteal, A. V. J. Edge and L. A. Woolf, J. Phys. Chem. **89**, 5318 (1985).

[94] M. Haughney, M. Ferrario and I. R. McDonald, Mol. Phys. **58**, 849 (1986).

[95] S. Z. Mikhail and W. R. Kimel, J. Chem. Eng. Data **6**, 533 (1961).

[96] H. Kubota, S. Tsuda, M. Murata, T. Yamamoto, Y. Tanaka, and T. Makita, Rev. Phys. Chem. Jpn. **49**, 59 (1979).

[97] J. D. Isdale, A. J. Easteal and L. A. Woolf, Int. J. Thermophys. **6**, 439 (1985).

[98] M. E. van Leeuwen and B. Smit, J. Phys. Chem. **99**, 1831 (1995).

[99] S. Dixit, W. C. K. Poon and J. Crain, J. Phys.: Condens. Matter **12**, L323 (2000).

[100] H. S. Frank and M. W. Evans, J. Chem. Phys. **13**, 507 (1945).

[101] S. Okazaki, H. Touhara and K. Nakanishi, J. Chem. Phys. **81**, 890 (1984).

[102] C. Corsaro, J. Spooren, C. Branca, N. Leone, M. Broccio, C. Kim, S. H. Chen, H. E. Stanley and F. Mallamace, J. Phys. Chem. B **112**, 10449 (2008).

[103] H. A. Zarei, F. Jalili and S. Assadi, J. Chem. Eng. Data **52**, 2517 (2007).

[104] M. L. McGlashan and A. G. Williamson, J. Chem. Eng. Data **21**, 196 (1976).

[105] R. F. Lama and B. C. Y. Lu, J. Chem. Eng. Data **10**, 216 (1965).

[106] K. R. Harris, P. J. Newitt and Z. J. Derlacki, J. Chem. Soc., Faraday Trans **94**, 1963 (1998).

[107] R. L. Kay and T. L. Broadwater, J. Sol. Chem. **5**, 57 (1976).

[108] Y. Tanaka, T. Yamamoto, Y. Satomi, H. Kubota and T. Makita, Rev. Phys. Chem. Jpn. **47**, 12 (1977).

[109] E. C. Bingham and R. F. Jackson, Bull. Bureau Standards **14**, 59 (1918).

[110] L. Saiz, J. A. Padró and E. Guàrdia, J. Phys. Chem. B **101**, 78 (1997).

[111] K. Mizuno, Y. Miyashita, Y. Shindo and H. Ogawa, J. Phys. Chem. **99**, 3225 (1995).

[112] K. Mizuno, Y. Kimura, H. Morichika, Y. Nishimura, S. Shimada, S. Maeda, S. Imafuji and T. Ochi, J. Mol. Liq. **85**, 139 (2000).

[113] J. A. Larkin, J. Chem. Thermodyn. **7**, 137 (1975).

[114] J. A. Boyne and A. G. Williamson, J. Chem. Eng. Data **12**, 318 (1967).

[115] M. E. van Leeuwen, Mol. Phys. **87**, 101 (1996).

[116] A. Perera, L. Zoranic, F. Sokolic and R. Mazighi, J. Mol. Liquids, doi: 10.1016/j.molliq.2010.05.006 (2010).

Table 1. Self-diffusion coefficient of pure liquid water from the literature, calculated at around 300 K and 0.1 MPa based on different molecular models. The number of particles is N. Different methods were applied: Mean square displacement (MSD), Green-Kubo (GK), Ewald summation (ES), particle mesh Ewald (PME), reaction field (RF) and force shifting (FS).

Model	Method	Electrostatics	N	T / K	D_i / $10^{-9}\mathrm{m}^2\mathrm{s}^{-1}$	Ref.
SPC	GK	ES	216	300	4.69	[11]
	MSD	RF	512	300	5.28	[12]
	MSD	PME	216	298.2	4.02	[13]
	MSD	RF	1000	300.7	4.2	[14]
	MSD	RF	820	301	4.5	[15]
	MSD	PME	2201	298.15	4.29	[16]
	MSD	RF	2201	298.15	2.71	[16]
	GK	ES	216	298	3.6	[17]
	MSD	FS	901	298.6	4.2	[18]
	MSD	na*	267	298.15	3.85	[19]
	GK	RF	2048	298.15	4.34	This work
SPC/E	na	na	216	300	2.5	[6]
	MSD	PME	216	298.2	2.41	[13]
	MSD	RF	1000	301	2.4	[14]
	MSD	RF	820	301	2.8	[15]
	MSD	PME	2201	298.15	2.7	[16]
	GK	ES	216	298	2.4	[17]
	MSD	FS	901	298.2	2.8	[18]
	MSD	na	267	298.15	2.49	[19]
	MSD	ES	256	298	2.58	[20]
	GK	ES	256	298	2.75	[20]
	GK	RF	2048	298.15	2.72	This work
TIP4P	MSD	ES	360	298	3.22	[9]
	MSD	RF	820	301	3.9	[15]
	MSD	RF	2201	298.15	3.02	[16]
	MSD	PME	2201	298.15	3.73	[16]
	GK	ES	216	298	3.3	[17]
	GK	RF	2048	298.15	3.69	This work
TIP4P/Ew	MSD	ES	512	297.4	2.4	[21]
TIP4P/2005	MSD	ES	360	298	2.07	[9]
	GK	RF	2048	298.15	2.25	This work

* not specified by the authors.

Table 2. Shear viscosity of for pure liquid water from the literature, calculated at around 300 K and 0.1 MPa based on different molecular models. The number of particles is N. Different methods were applied: Equilibrium molecular dynamics (EMD), non-equilibrium molecular dynamics (NEMD), Ewald summation (ES), particle mesh Ewald (PME) and reaction field (RF).

Model	Method	Electrostatics	N	T K	η 10^{-4}Pa s	Ref.
SPC	EMD	RF	512	300	5.8	[12]
	NEMD	PME	864	300.2	4.0	[13]
	EMD	RF	1000	300.7	4.9	[14]
	NEMD	PME	3456	300	4.0	[23]
	NEMD	RF	3456	300	4.0	[23]
	EMD	RF	2048	298.15	4.9	This work
SPC/E	EMD	RF	512	301	9.1	[12]
	NEMD	PME	864	300.2	7.2	[13]
	EMD	RF	1000	300.7	4.9	[14]
	NEMD	PME	6912	300	6.4	[23]
	EMD	ES	512	303.15	6.6	[25]
	NEMD	ES	512	303.15	6.2	[25]
	EMD	ES	224	298	6.6	[26]
	EMD	ES	256	303	6.5	[27]
	EMD	PME	500	298	7.3	[28]
	NEMD	ES	300	298.15	7.5	[55]
	EMD	RF	2048	298.15	8.2	This work
TIP4P	NEMD	PME	1000	298	4.8	[4]
	NEMD	PME	1000	298	4.6	[4]
	EMD	PME	500	298	4.9	[28]
	EMD	na*	343	298	4.7	[29]
	EMD	RF	2048	298.15	5.6	This work
TIP4P/2005	EMD	PME	500	298	8.6	[28]
	EMD	RF	2048	298.15	8.9	This work

* not specified by the authors.

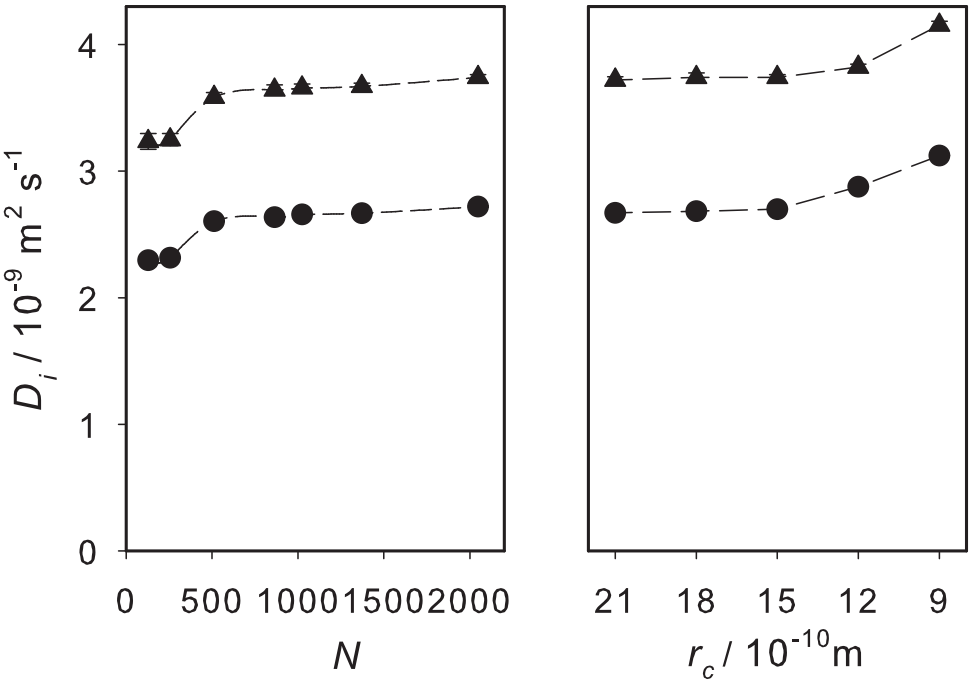

Figure 1. System size (left) and cut-off radius (right) dependence of the predicted self-diffusion coefficient of pure liquid water at 298.15 K and 0.1 MPa. Present simulation results are shown for the SPC/E (•) and TIP4P (▲) models. Lines are drawn as a guide to the eye.

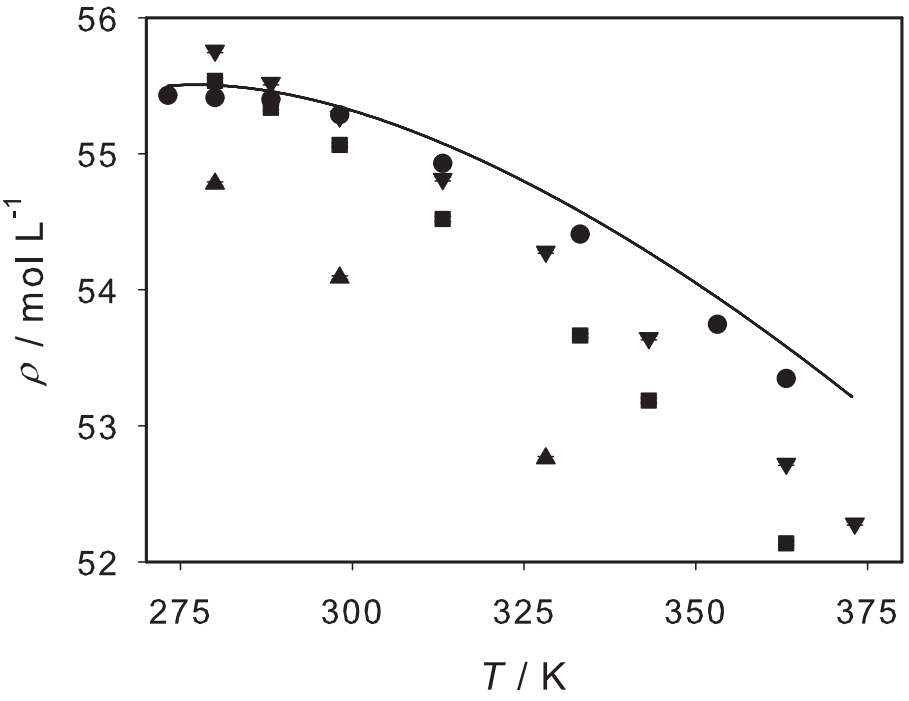

Figure 2. Temperature dependence of the predicted density of pure liquid water at 0.1 MPa. Present simulation results are shown for the SPC (▲), SPC/E (▼), TIP4P (■) and TIP4P/2005 (•) models in comparison to a correlation of experimental data (−) [70].

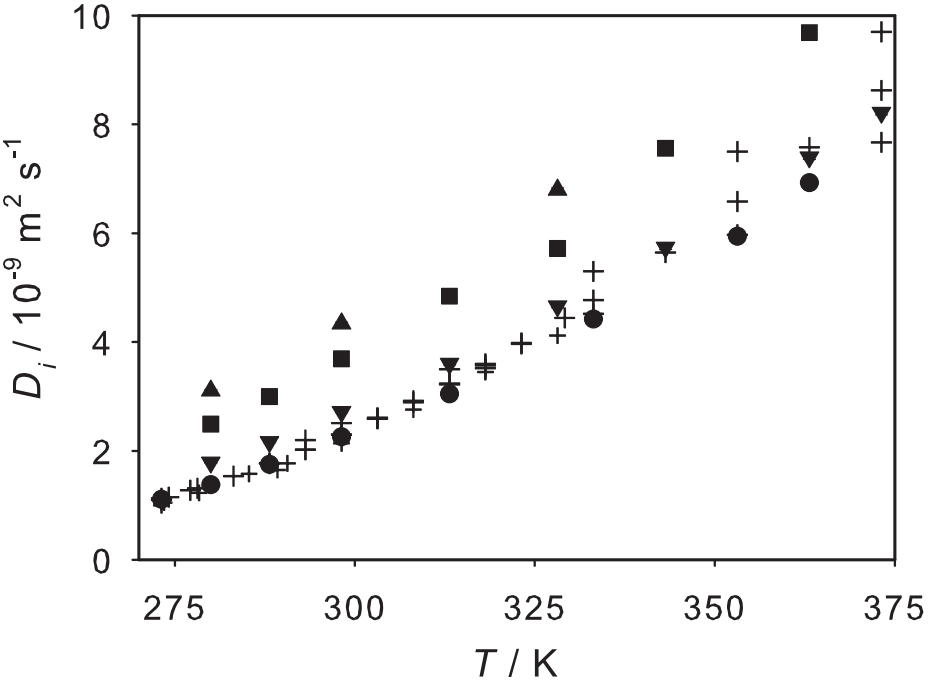

Figure 3. Temperature dependence of the predicted self-diffusion coefficient of pure liquid water at 0.1 MPa. Present simulation results are shown for the SPC (▲), SPC/E (▼), TIP4P (■) and TIP4P/2005 (●) models in comparison to experimental data (+) [71–77].

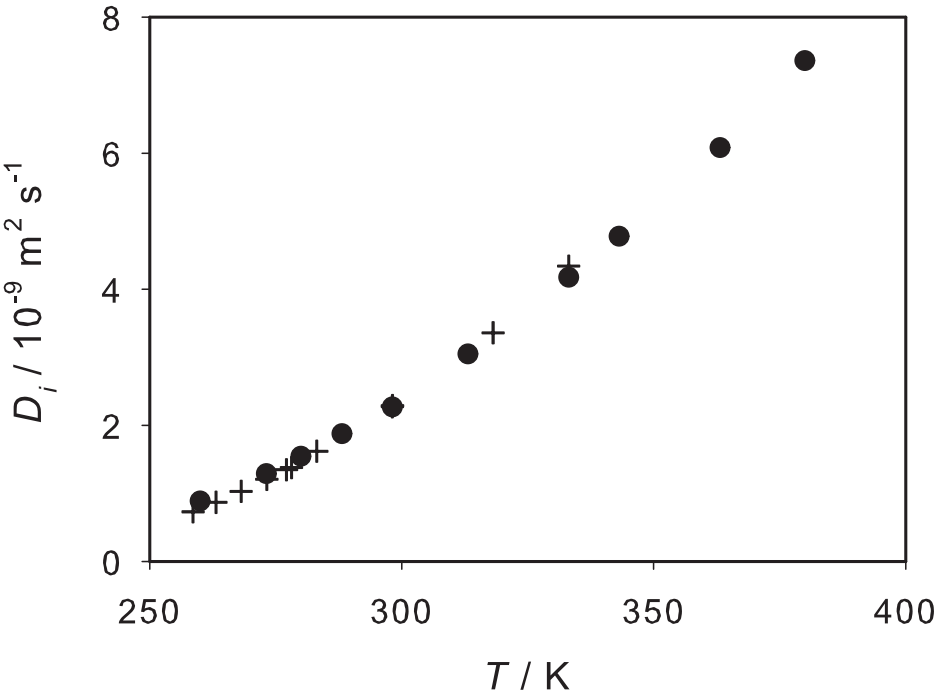

Figure 4. Temperature dependence of the predicted shear viscosity of pure liquid water at 200 MPa. Present simulation results for the TIP4P/2005 (•) model are shown in comparison to experimental data (+) [74, 78, 79].

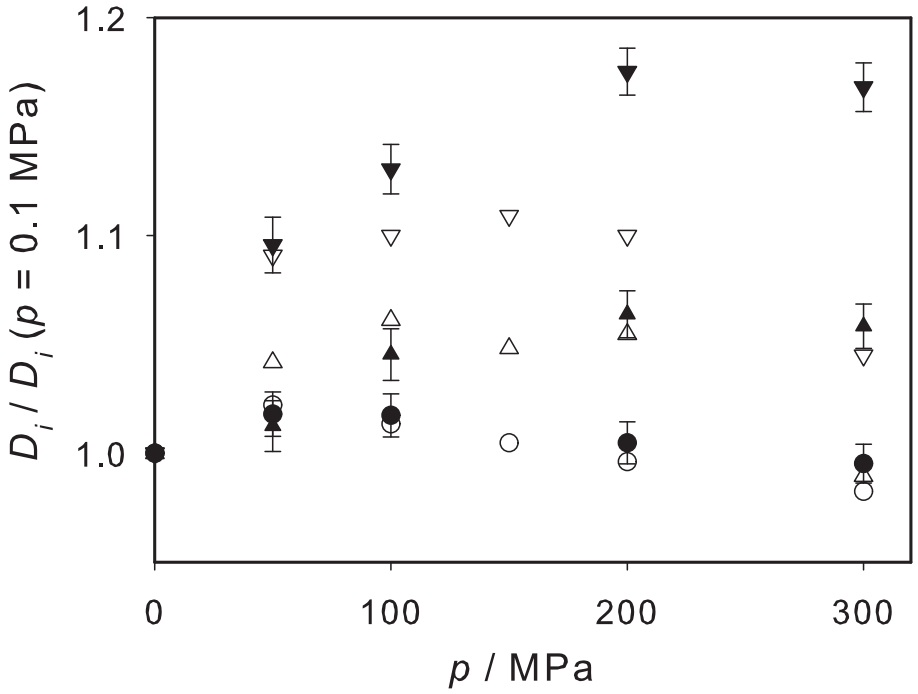

Figure 5. Pressure dependence of the predicted self-diffusion coefficient of pure liquid water at 273.15 K (▼), 280 K (▲) and 298.15 K (●). Present simulation results for the TIP4P/2005 model are shown in comparison to experimental data at 274.15 K (▽), 283.15 K (△) and 298.15 K (○) [74, 78].

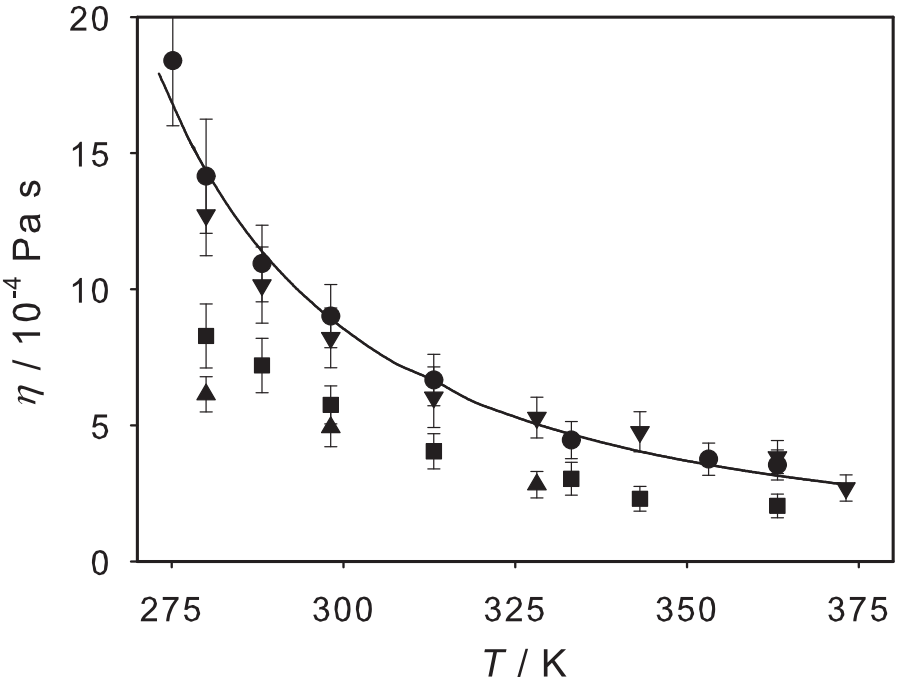

Figure 6. Temperature dependence of the predicted shear viscosity of pure liquid water at 0.1 MPa. Present simulation results for the SPC (▲), SPC/E (▼), TIP4P (■) and TIP4P/2005 (•) models are shown in comparison to a correlation of experimental data (−) [86].

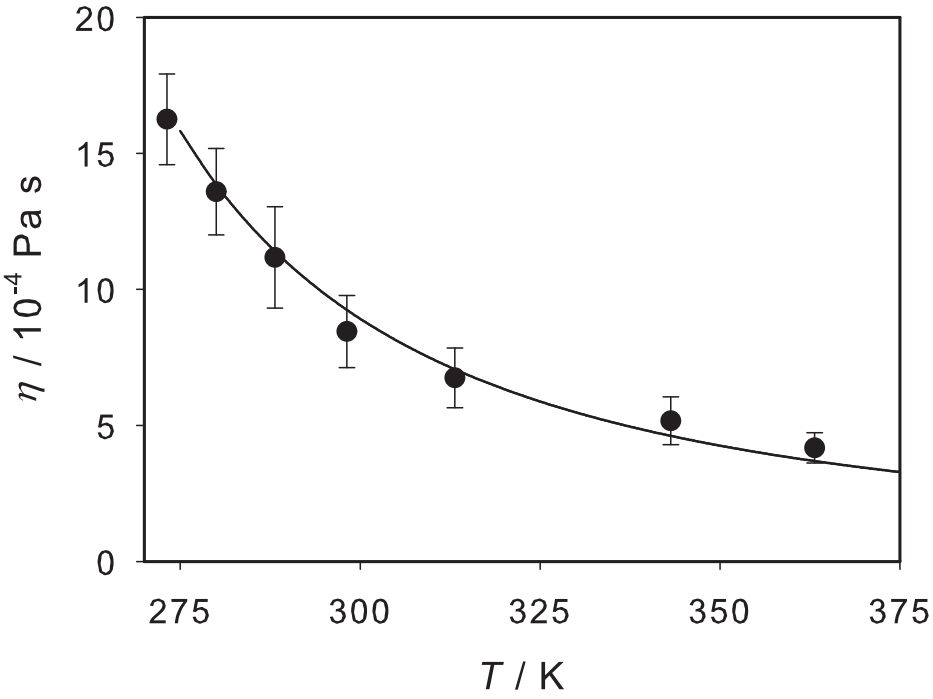

Figure 7. Temperature dependence of the predicted shear viscosity of pure liquid water at 200 MPa. Present simulation results for the TIP4P/2005 (•) model are shown in comparison to a correlation of experimental data (+) [86].

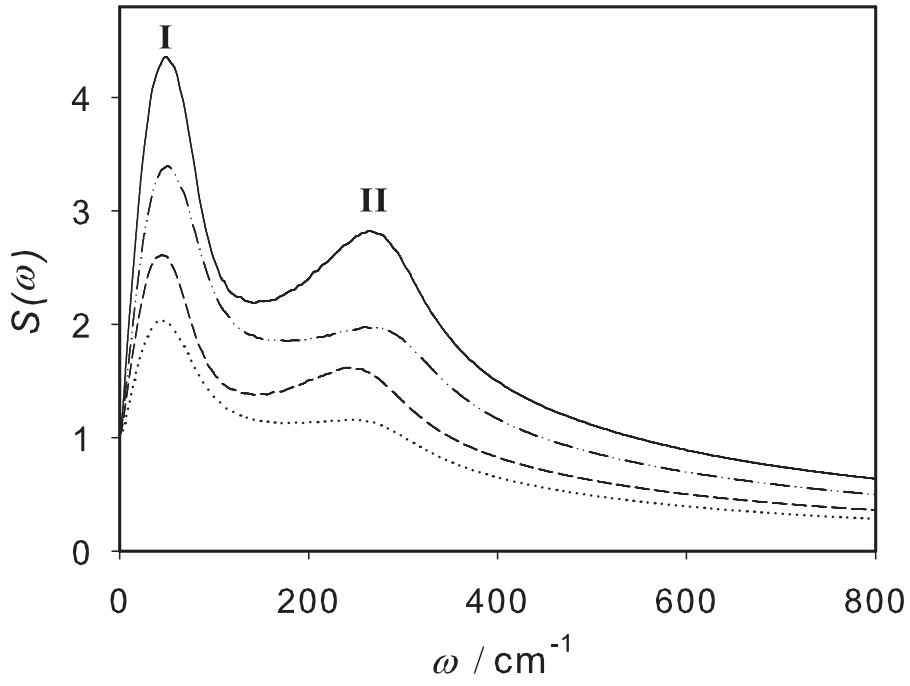

Figure 8. Normalized power spectrum of pure liquid water at 280 K and 0.1 MPa for the SPC ($\cdots$), SPC/E ($--$), TIP4P($- \cdot -$) and TIP4P/2005 ($-$) models.

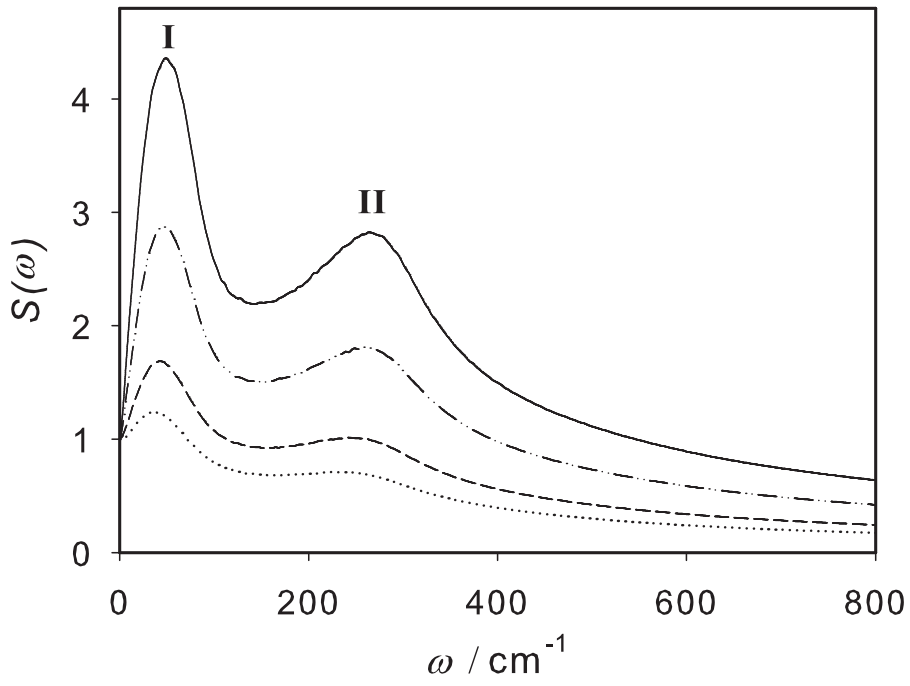

Figure 9. Normalized power spectrum of pure liquid water at 0.1 MPa and 280 K (−), 298.15 K (− · −), 333.15 K (−−) and 363.15 K (· · ·) for the TIP4P/2005 model.

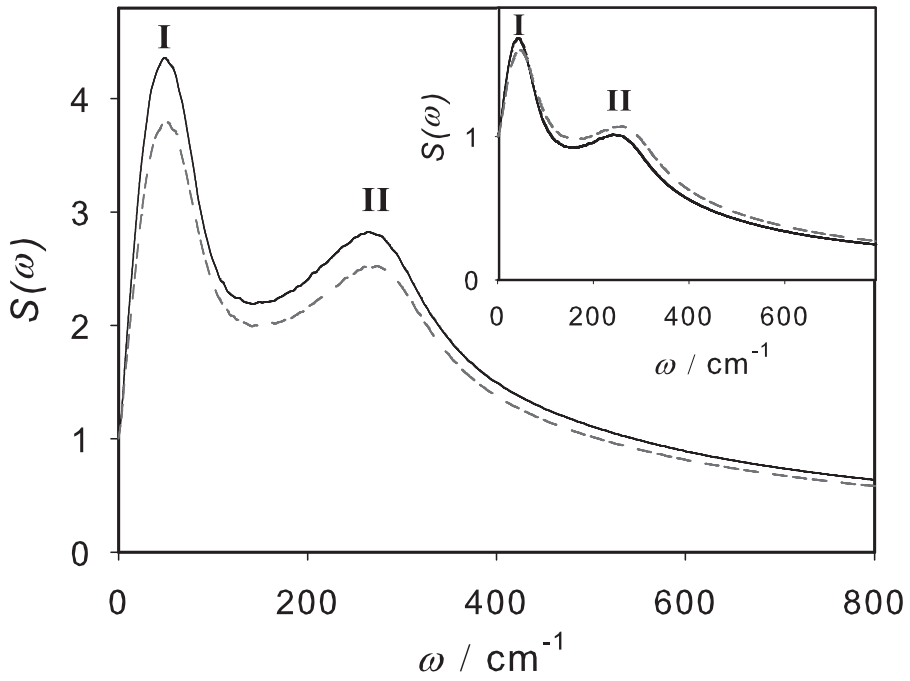

Figure 10. Normalized power spectrum of pure liquid water at 280 K and 333.15 K (inset) and at 0.1 MPa (−) and 300 MPa (−−) for the TIP4P/2005 model.

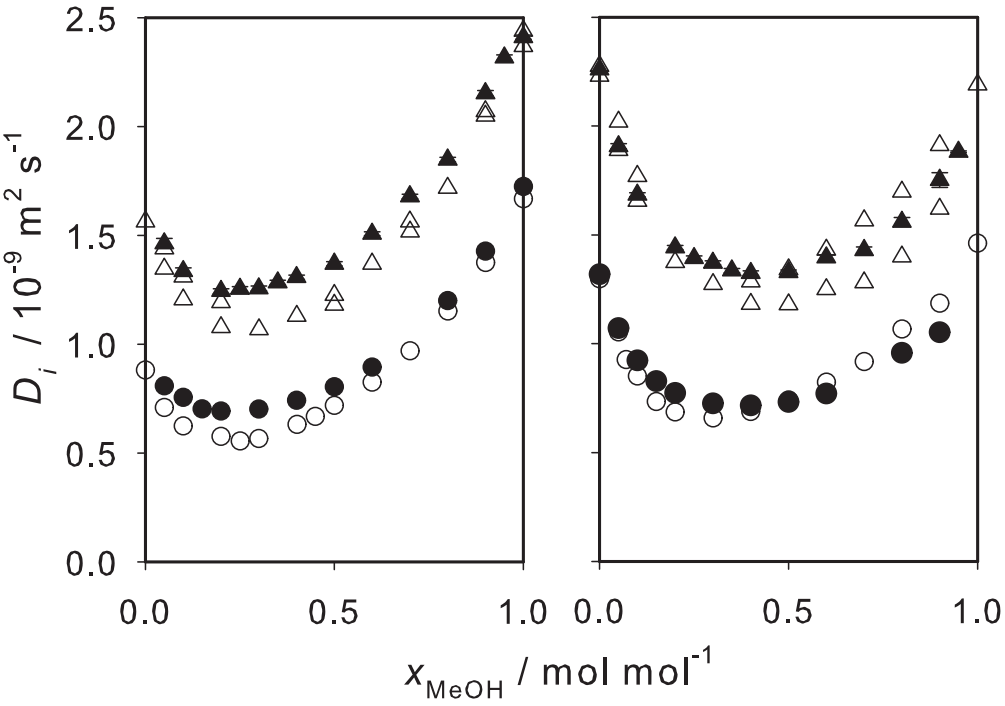

Figure 11. Self-diffusion coefficient of methanol (left) and water (right) in their binary mixture at 0.1 MPa and 278.15 K (•) as well as 298.15 K (▲). Present simulation results for the TIP4P/2005 model (full symbols) are compared to experimental data (empty symbols) [45, 93].

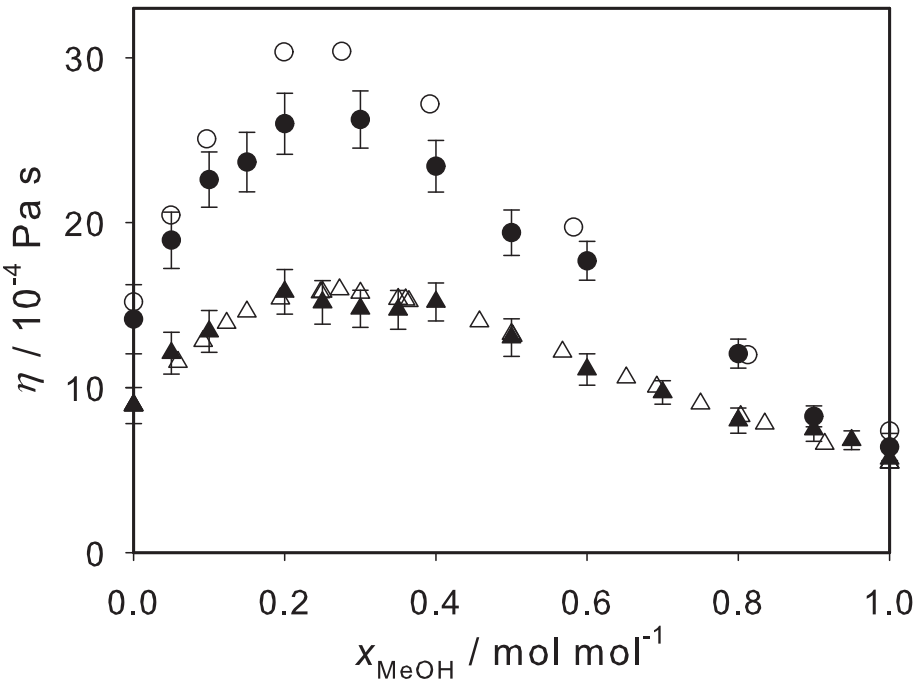

Figure 12. Shear viscosity of the mixture water + methanol at 0.1 MPa and 278.15 K (•) as well as 298.15 K (▲). Present simulation results for the TIP4P/2005 model (full symbols) are compared to experimental data (empty symbols) [95–97].

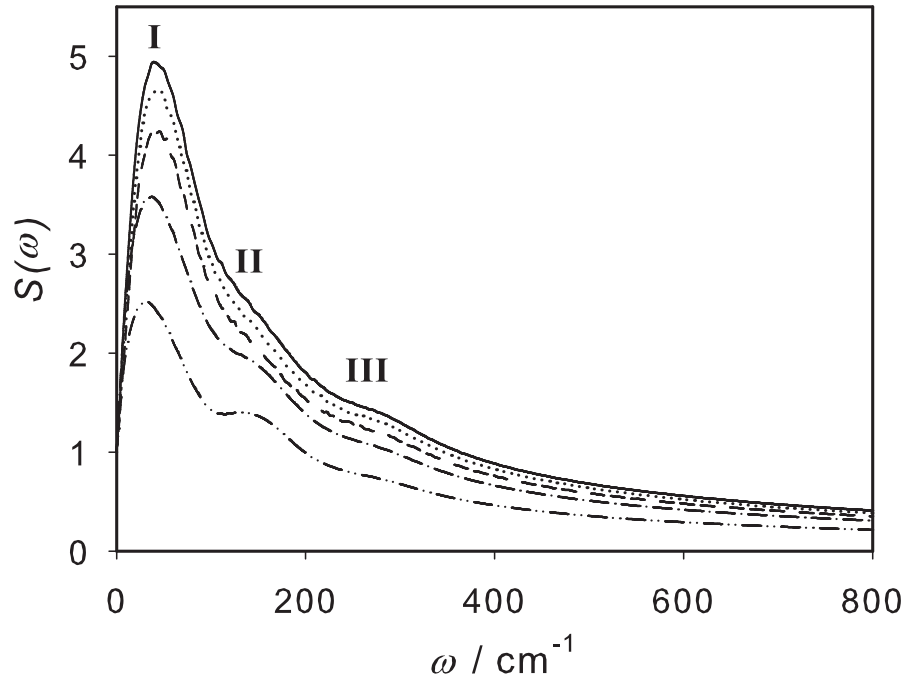

Figure 13. Normalized power spectrum of pure methanol and methanol in its aqueous mixture at 298.15 K, 0.1 MPa and $x_{\mathrm{MeOH}} = 0.05$ mol/mol (−−), 0.1 mol/mol (···), 0.3 mol/mol (−), 0.7 mol/mol (− · −) and 1 mol/mol (− ··−).

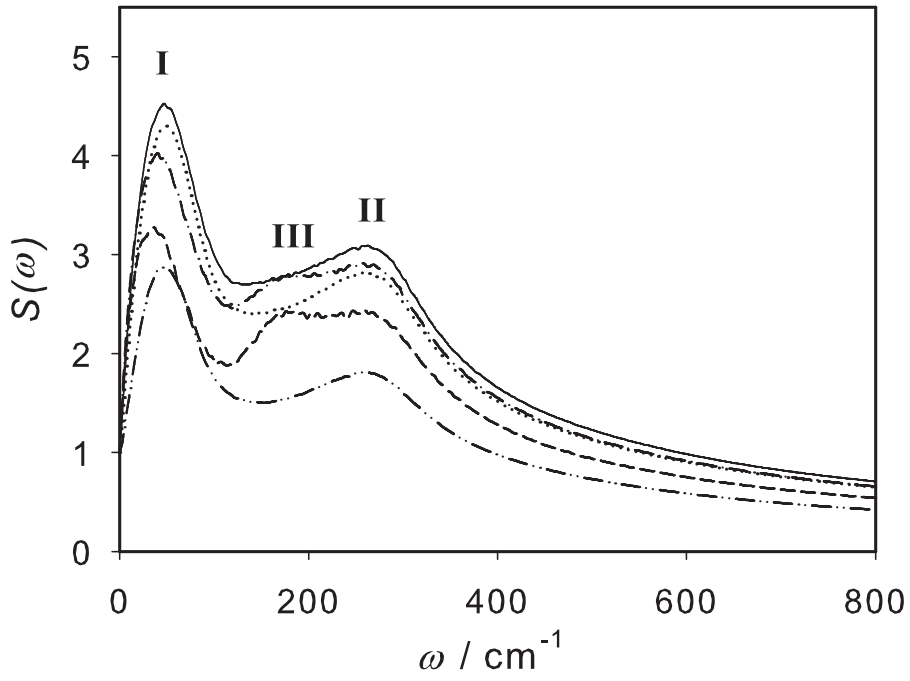

Figure 14. Normalized power spectrum of pure water and water in its mixture with methanol at 298.15 K, 0.1 MPa and $x_{\mathrm{MeOH}} = 0$ mol/mol ($- \cdot\cdot -$), 0.2 mol/mol ($\cdots$), 0.4 mol/mol ($-$), 0.6 mol/mol ($- \cdot -$) and 0.9 mol/mol ($--$).

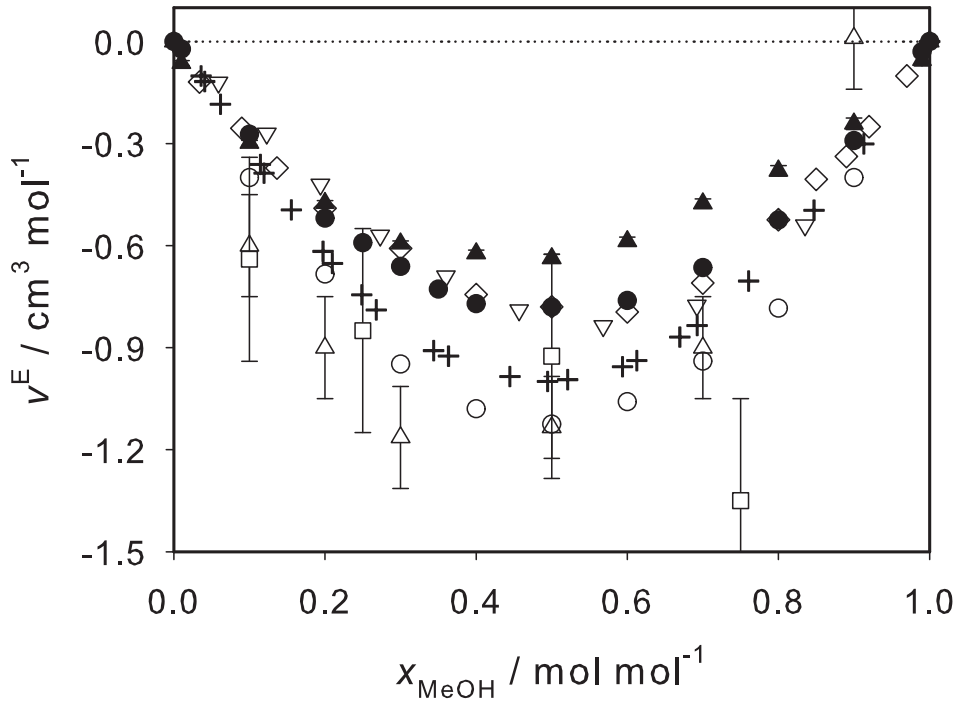

Figure 15. Excess volume of water + methanol at 298.15 K and 0.1 MPa. Present simulation results for the TIP4P/2005 (•) and SPC/E (▲) models are compared to simulation results from the literature (○) [41], (◊) [51], (△) [52], (▽) [4], (□) [54] and experimental data (+) [103, 104].

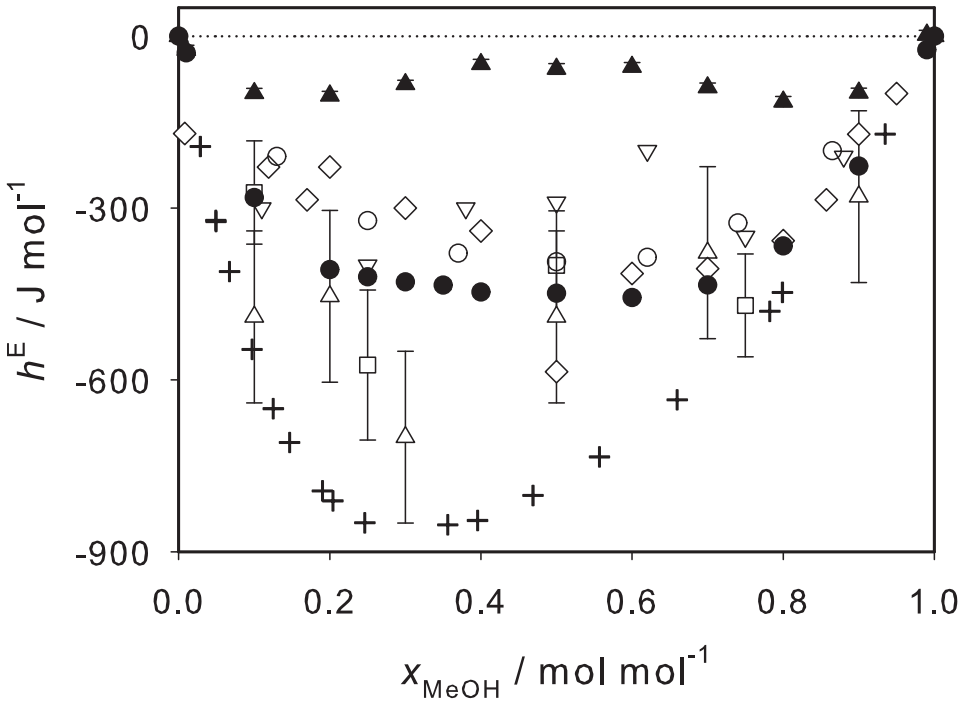

Figure 16. Excess enthalpy of water + methanol at 298.15 K and 0.1 MPa. Present simulation results for the TIP4P/2005 (•) and SPC/E (▲) models are compared to simulation results from the literature (○) [41], (◊) [51], (△) [52], (▽) [53], (□) [54] and experimental data (+) [105].

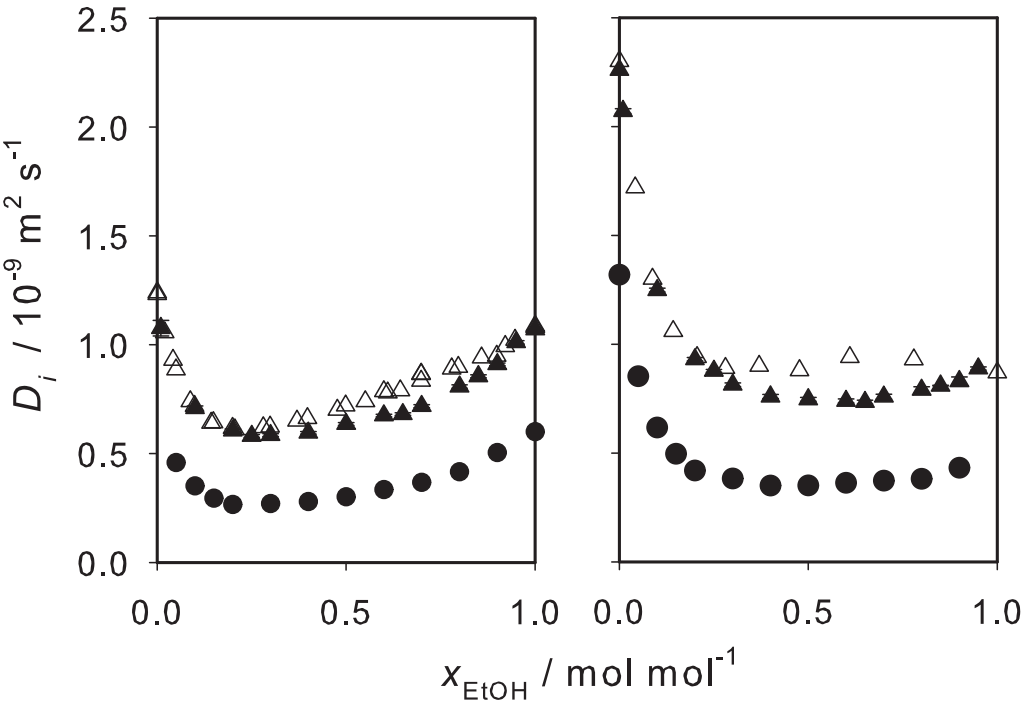

Figure 17. Self-diffusion coefficient of ethanol (left) and water (right) in their binary mixture at 0.1 MPa and 278.15 K (•) as well as 298.15 K (▲). Present simulation results for the TIP4P/2005 model (full symbols) are compared to experimental data (empty symbols) as far as available [40, 106].

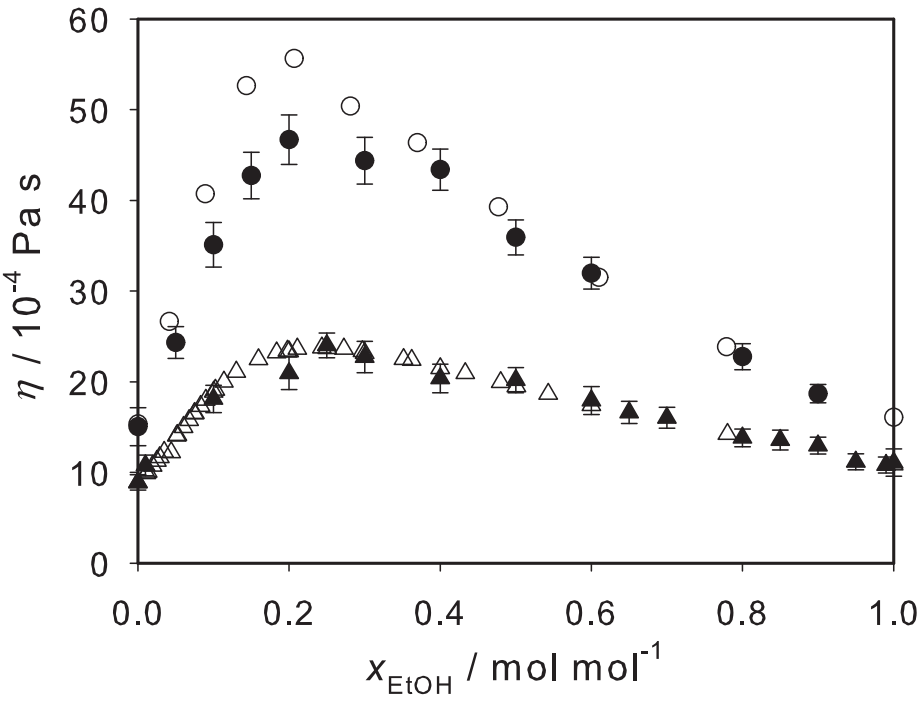

Figure 18. Shear viscosity of the mixture water + ethanol at 0.1 MPa and 278.15 K (●) as well as 298.15 K (▲). Present simulation results for the TIP4P/2005 model (full symbols) are compared to experimental data (empty symbols) [103, 107–109].

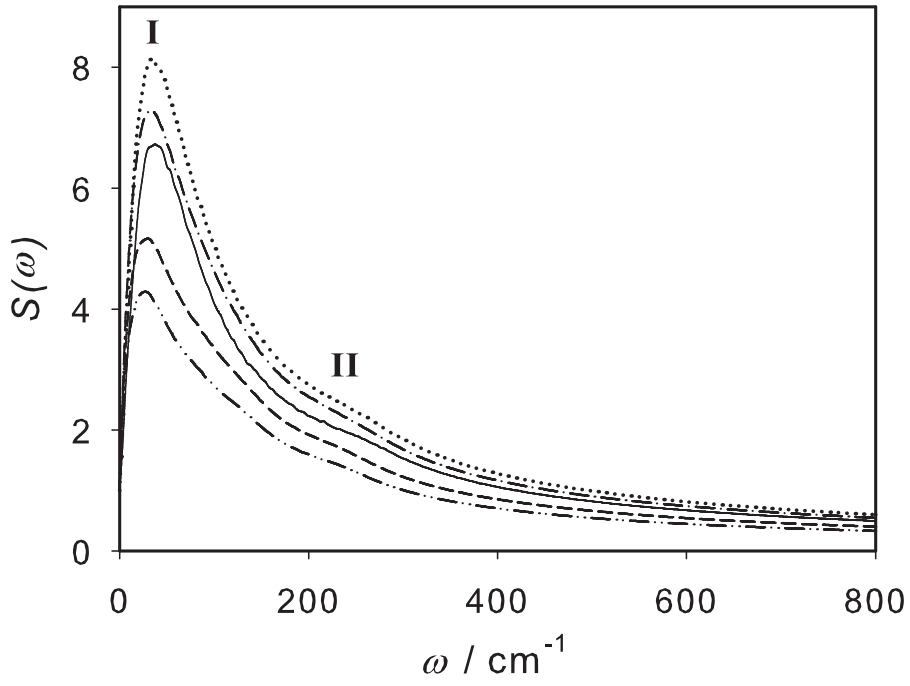

Figure 19. Normalized power spectrum of pure ethanol and ethanol in its aqueous mixture at 298.15 K, 0.1 MPa and $x_{\mathrm{EtOH}} = 0.1$ mol/mol (−), 0.25 mol/mol (· · ·), 0.5 mol/mol (− · −), 0.9 mol/mol (− −) and 1 mol/mol (− · · −).

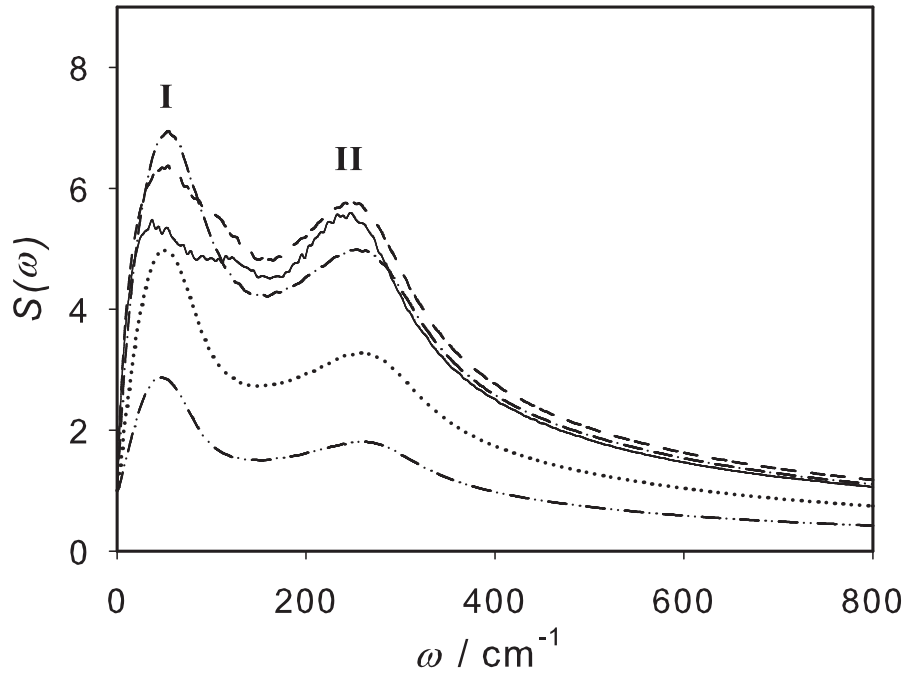

Figure 20. Normalized power spectrum of pure water and water in its mixture with ethanol at 298.15 K, 0.1 MPa and $x_{\mathrm{EtOH}} = 0$ mol/mol ($-\cdots-$), 0.1 mol/mol ($\cdots$), 0.3 mol/mol ($- \cdot -$), 0.6 mol/mol ($--$) and 0.9 mol/mol ($- \cdot -$).

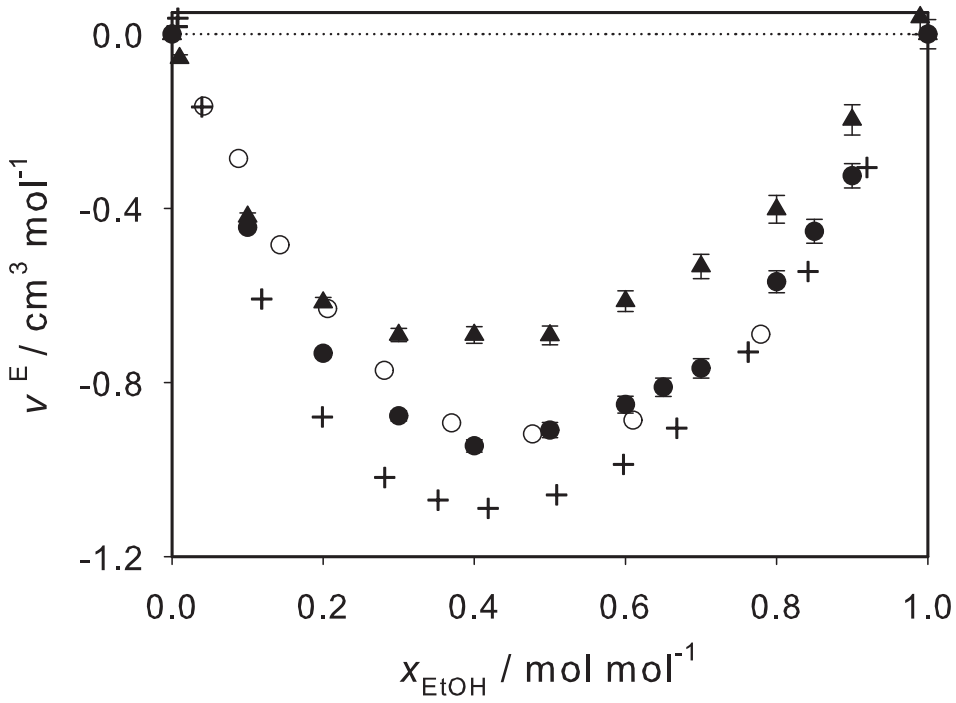

Figure 21. Excess volume of the mixture water + ethanol at 298.15 K and 0.1 MPa. Present simulation results for the TIP4P/2005 (•) and SPC/E (▲) models are compared to simulation results from the literature (○) [4] and experimental data (+) [103].

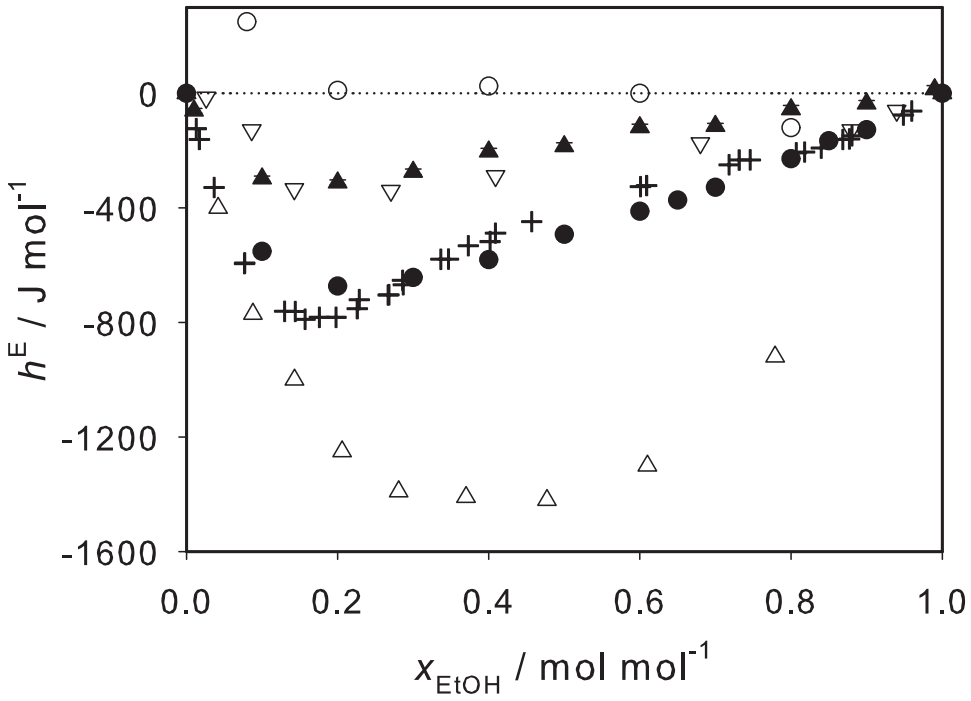

Figure 22. Excess enthalpy of the mixture water + ethanol at 298 K and 0.1 MPa. Present simulation results for the TIP4P/2005 (•) and SPC/E (▲) models are compared to simulation results from the literature (○) [49], (△) [4], (▽) [50] and experimental data (+) [105, 114].

Supplemental material to:

Prediction of self-diffusion coefficient and shear viscosity of water and its binary mixtures with methanol and ethanol by molecular simulation

by: Gabriela Guevara-Carrion, Jadran Vrabec and Hans Hasse

Table 1. Self-diffusion coefficient and shear viscosity of pure liquid water from present NVT simulations based on different molecular models. The densities were chosen to yield a pressure of 0.1 MPa. The number in parentheses indicates the statistical uncertainty in the last digit.

T K	ρ mol l^{-1}	D_i $10^{-9}m^2s^{-1}$	η 10^{-4}Pa s
SPC			
280	54.78	3.11 (2)	6.1 (7)
298.15	54.09	4.34 (3)	4.9 (6)
328.15	52.76	6.80 (4)	2.8 (4)
SPC/E			
280	55.76	1.79 (1)	13 (1)
288.15	55.52	2.17 (1)	10 (1)
298.15	55.27	2.72 (2)	8.2 (9)
313.15	54.82	3.60 (2)	6.0 (7)
328.15	54.28	4.66 (3)	5.3 (7)
343.15	53.65	5.74 (4)	4.8 (6)
363.15	52.72	7.39 (4)	3.8 (5)
373.15	52.28	8.21 (4)	2.7 (4)
TIP4P			
280	55.54	2.49 (2)	8 (1)
288.15	55.34	3.00 (2)	7.2 (8)
298.15	55.06	3.69 (2)	5.6 (7)
313.15	54.52	4.84 (2)	4.0 (6)
333.15	53.67	5.72 (3)	3.0 (5)
343.15	53.19	7.56 (4)	2.2 (4)
363.15	52.14	9.69 (5)	2.0 (3)
TIP4P/2005			
273.15	55.43	1.11 (1)	18 (2)
280	55.41	1.38 (1)	14 (2)
288.15	55.40	1.75 (1)	11 (1)
298.15	55.29	2.26 (2)	8.9 (9)
313.15	54.92	3.05 (2)	6.7 (7)
333.15	54.41	4.42 (3)	4.5 (6)
353.15	53.74	5.94 (3)	3.8 (5)
363.15	53.35	6.93 (4)	3.5 (5)

Table 2. Self-diffusion coefficient and shear viscosity of pure liquid water from present NVT simulations based on the TIP4P/2005 model at different temperatures and pressures. The densities were chosen to yield the given pressures. The number in parentheses indicates the statistical uncertainty in the last digit.

T K	ρ mol l^{-1}	D_i $10^{-9}m^2s^{-1}$	η 10^{-4}Pa s
$p = 50$ MPa			
260	56.68	0.770 (7)	–
273.15	54.73	1.22 (1)	16 (2)
280	56.73	1.47 (1)	16 (2)
288.15	56.64	1.77 (1)	14 (1)
298.15	56.47	2.30 (2)	9.9 (9)
313.15	56.19	3.10 (2)	8.1 (8)
333.15	55.62	4.34 (3)	5.2 (7)
343.15	55.30	5.04 (3)	4.6 (7)
363.15	54.59	6.62 (4)	4.3 (6)
380	53.95	3.49 (6)	3.5 (5)
$p = 100$ MPa			
260	57.97	0.837 (7)	–
273.15	57.96	1.261 (9)	16 (2)
280	57.87	1.52 (1)	14 (1)
288.15	57.72	1.86 (1)	8.7 (9)
298.15	57.60	2.30 (2)	7.9 (9)
313.15	57.26	3.09 (2)	7.6 (8)
333.15	56.70	4.32 (3)	6.2 (7)
343.15	56.42	4.97 (3)	5.4 (6)
363.15	55.77	6.49 (4)	4.0 (5)
380	55.14	7.77 (4)	3.8 (5)
400	54.33	7.77 (4)	2.7 (4)

Continued on next page

Table 2 – continued from previous page

T K	ρ mol l^{-1}	D_i $10^{-9}m^2s^{-1}$	η 10^{-4}Pa s
$p = 200$ MPa			
260	60.22	0.890 (8)	–
273.15	60.06	1.310 (9)	16 (2)
280	59.86	1.55 (1)	14 (1)
288.15	59.77	1.88 (1)	12 (1)
298.15	59.55	2.27 (1)	8.3 (9)
313.15	59.21	3.05 (2)	6.8 (8)
333.15	58.65	4.18 (2)	6.0 (8)
343.15	58.33	4.78 (3)	5.7 (7)
363.15	57.69	6.08 (3)	4.2 (6)
380	57.12	7.36 (4)	3.1 (5)
400	56.40	8.94 (4)	3.0 (5)
$p = 300$ MPa			
260	62.10	0.897 (9)	–
273.15	61.80	1.30 (1)	18 (2)
280	61.66	1.54 (1)	16 (2)
288.15	61.43	1.86 (1)	15 (1)
298.15	61.22	2.28 (1)	10 (1)
313.15	60.82	2.97 (2)	7.8 (9)
333.15	60.26	4.05 (2)	5.5 (7)
363.15	59.35	5.86 (3)	4.1 (6)
373.15	59.04	6.47 (4)	3.9 (6)
400	58.14	8.38 (5)	2.3 (4)

Table 3. Self-diffusion coefficient and shear viscosity of the mixture water + methanol at 298.15 K from present NVT simulations based on the SPC/E and TIP4P/2005 water models as well as the methanol model by Schnabel et al. The densities were chosen to yield a pressure of 0.1 MPa. The number in parentheses indicates the statistical uncertainty in the last digit.

x_{MeOH}	ρ	D_{MeOH}	D_{W}	η
mol mol^{-1}	mol l^{-1}	10^{-9}m^{2}s^{-1}	10^{-9}m^{2}s^{-1}	10^{-4}Pa s
SPC/E				
0	55.27		2.72 (2)	8.2 (9)
0.01	54.77	1.95 (6)	2.55 (2)	9.2 (9)
0.10	49.84	1.71 (2)	2.18 (1)	11 (1)
0.20	45.13	1.64 (2)	1.97 (1)	10 (1)
0.30	41.13	1.60 (2)	1.81 (2)	12 (1)
0.40	37.66	1.64 (1)	1.78 (1)	10 (1)
0.50	34.71	1.67 (2)	1.74 (2)	9.2 (9)
0.60	32.12	1.76 (1)	1.73 (2)	9.6 (9)
0.70	29.84	1.89 (1)	1.78 (2)	8.4 (8)
0.80	27.86	2.04 (1)	1.85 (2)	7.6 (8)
0.90	26.12	2.25 (1)	1.92 (4)	5.7 (7)
0.99	24.67	2.46 (1)	1.93 (6)	4.3 (6)
1	24.53	2.41 (2)		5.7 (6)
TIP4P/2005				
0	55.29		2.26 (2)	8.9 (9)
0.05	52.41	1.46 (2)	1.91 (1)	12 (1)
0.10	49.80	1.34 (2)	1.69 (1)	13 (1)
0.20	45.25	1.24 (1)	1.44 (1)	16 (2)
0.25	43.17	1.25 (1)	1.39 (1)	15 (2)
0.30	41.28	1.26 (1)	1.37 (1)	15 (2)
0.35	39.52	1.28 (1)	1.34 (1)	15 (2)
0.40	37.90	1.31 (1)	1.32 (1)	15 (2)
0.50	34.92	1.37 (1)	1.33 (1)	13 (1)
0.60	32.34	1.51 (1)	1.40 (1)	11 (1)
0.70	30.04	1.68 (1)	1.43 (1)	9.7 (9)
0.80	28.01	1.85 (1)	1.56 (2)	8.0 (9)
0.90	26.18	2.15 (1)	1.75 (3)	7.5 (8)
0.95	25.30	2.32 (1)	1.88 (4)	6.8 (8)
1	24.53	2.41 (2)		5.7 (6)

Table 4. Volume, excess volume, enthalpy and excess enthalpy of the mixture water + methanol at 298.15 K and 0.1 MPa from present NpT simulations on the basis of the SPC/E and TIP4P/2005 water models as well as the methanol model by Schnabel et al. The number in parentheses indicates the statistical uncertainty in the last digit.

x_{MeOH}	v	v^{E}	h	h^{E}
mol mol^{-1}	cm^{-3} mol^{-1}	cm^{-3} mol^{-1}	kJ mol^{-1}	J mol^{-1}
SPC/E				
0	18.092 (5)		−49.223 (4)	
0.01	18.256 (5)	−0.063 (7)	−49.154 (7)	−24 (8)
0.10	20.065 (5)	−0.298 (7)	−48.392 (7)	−99 (9)
0.20	22.160 (6)	−0.475 (8)	−47.467 (6)	−104 (8)
0.30	24.314 (6)	−0.594 (8)	−46.517 (6)	−84 (7)
0.40	26.556 (6)	−0.622 (7)	−45.551 (8)	−49 (8)
0.50	28.313 (7)	−0.637 (8)	−44.630 (7)	−57 (9)
0.60	31.135 (7)	−0.587 (8)	−43.696 (7)	−54 (8)
0.70	33.518 (7)	−0.476 (8)	−42.802 (7)	−90 (8)
0.80	35.894 (8)	−0.371 (9)	−41.896 (8)	−114 (9)
0.90	38.295 (8)	−0.242 (9)	−40.951 (7)	−99 (8)
0.99	40.527 (9)	−0.05 (1)	−40.013 (6)	+2 (8)
1	40.753 (7)		−39.922 (5)	
TIP4P/2005				
0	18.087 (6)		−50.288 (4)	
0.01	18.292 (5)	−0.022 (8)	−50.213 (6)	−29 (7)
0.10	20.081 (4)	−0.273 (7)	−49.533 (5)	−282 (6)
0.20	22.101 (4)	−0.520 (6)	−48.622 (5)	−408 (7)
0.25	23.162 (6)	−0.592 (8)	−48.117 (7)	−420 (8)
0.30	24.226 (5)	−0.661 (7)	−47.607 (5)	−429 (6)
0.35	25.304 (6)	−0.716 (8)	−47.094 (7)	−435 (7)
0.40	26.383 (5)	−0.771 (6)	−46.588 (6)	−447 (7)
0.50	28.639 (6)	−0.781 (7)	−45.554 (5)	−449 (6)
0.60	30.925 (6)	−0.761 (8)	−44.525 (5)	−456 (6)
0.70	33.288 (6)	−0.665 (8)	−43.466 (6)	−434 (7)
0.80	35.695 (6)	−0.525 (8)	−42.361 (5)	−366 (6)
0.90	38.195 (7)	−0.291 (9)	−41.186 (6)	−227 (7)
0.99	40.506 (8)	−0.02 (1)	−40.028 (6)	−2 (8)
1	40.753 (7)		−39.922 (5)	

Table 5. Self-diffusion coefficient and shear viscosity of the mixture water + ethanol at 298.15 K from present NVT simulations based on the SPC/E and TIP4P/2005 water models as well as the ethanol model by Schnabel et al. The densities were chosen to yield a pressure of 0.1 MPa. The number in parentheses indicates the statistical uncertainty in the last digit.

x_{EtOH}	ρ	D_{EtOH}	D_{W}	η
mol mol^{-1}	mol l^{-1}	10^{-9}m^{2}s^{-1}	10^{-9}m^{2}s^{-1}	10^{-4}Pa s
SPC/E				
0	55.27		2.72 (2)	8.2 (9)
0.01	54.23	1.46 (6)	2.55 (2)	7.9 (9)
0.10	46.07	0.99 (1)	1.68 (1)	12 (1)
0.20	39.15	0.83 (1)	1.33 (1)	19 (2)
0.30	33.89	0.794 (9)	1.14 (1)	21 (2)
0.40	29.80	0.760 (8)	1.04 (1)	20 (2)
0.50	26.62	0.767 (9)	0.98 (1)	18 (2)
0.60	23.99	0.777 (8)	0.92 (1)	16 (2)
0.70	21.84	0.812 (1)	0.90 (2)	15 (2)
0.80	20.02	0.867 (8)	0.89 (1)	14 (1)
0.90	18.45	0.899 (9)	0.84 (2)	12 (1)
0.99	17.22	1.014 (9)	0.93 (6)	11 (1)
1	17.11	1.07 (1)		11 (1)
TIP4P/2005				
0	55.29		2.26 (2)	8.9 (9)
0.01	54.16	1.08 (4)	2.07 (1)	11 (1)
0.10	46.13	0.71 (1)	1.25 (1)	18 (2)
0.20	39.33	0.606 (7)	0.931 (8)	21 (2)
0.25	36.54	0.579 (6)	0.878 (7)	25 (3)
0.30	34.11	0.585 (6)	0.814 (8)	23 (3)
0.40	30.05	0.594 (6)	0.760 (8)	20 (2)
0.50	26.77	0.635 (6)	0.747 (9)	18 (2)
0.60	24.13	0.675 (6)	0.739 (9)	17 (2)
0.65	22.99	0.681 (5)	0.735 (9)	16 (2)
0.70	21.94	0.718 (6)	0.759 (9)	16 (2)
0.80	20.08	0.808 (7)	0.79 (1)	14 (1)
0.85	19.25	0.855 (7)	0.81 (2)	15 (2)
0.90	18.49	0.909 (6)	0.83 (2)	13 (1)
0.99	17.24	1.06 (7)	0.89 (7)	12 (1)
1	17.11	1.07 (1)		11 (1)

Table 6. Volume, excess volume, enthalpy and excess enthalpy of the mixture water + ethanol at 298.15 K and 0.1 MPa from present NpT simulations on the basis of the SPC/E and TIP4P/2005 water models as well as the ethanol model by Schnabel et al. The numbers in parentheses indicate the statistical uncertainty in the last digits.

x_{EtOH}	v	v^{E}	h	h^{E}
mol mol^{-1}	cm^{-3} mol^{-1}	cm^{-3} mol^{-1}	kJ mol^{-1}	J mol^{-1}
SPC/E				
0	18.092 (5)		−49.223 (4)	
0.10	21.707 (6)	−0.420 (8)	−48.647 (6)	−300 (8)
0.20	25.544 (7)	−0.618 (9)	−48.387 (8)	−315 (9)
0.30	29.503 (7)	−0.69 (1)	−47.776 (9)	−280 (10)
0.40	33.537 (8)	−0.69 (2)	−47.131 (9)	−211 (10)
0.50	37.570 (9)	−0.70 (2)	−46.538 (9)	−194 (10)
0.60	41.683 (9)	−0.62 (2)	−45.898 (9)	−130 (11)
0.70	45.796 (9)	−0.54 (3)	−45.321 (8)	−128 (10)
0.80	49.96 (1)	−0.41 (3)	−44.688 (8)	−71 (11)
0.90	54.20 (1)	−0.20 (3)	−44.094 (8)	−54 (11)
1	58.44 (1)		−43.465 (8)	
TIP4P/2005				
0	18.087 (6)		−50.288 (4)	
0.10	21.678 (4)	−0.445 (7)	−50.159 (6)	−554 (7)
0.20	25.423 (5)	−0.735 (9)	−49.600 (7)	−677 (8)
0.30	29.314 (6)	−0.88 (1)	−48.890 (7)	−649 (8)
0.40	33.279 (8)	−0.95 (1)	−48.147 (7)	−589 (8)
0.50	37.355 (9)	−0.91 (2)	−47.378 (9)	−502 (10)
0.60	41.443 (8)	−0.86 (2)	−46.617 (7)	−423 (9)
0.65	43.506 (9)	−0.81 (2)	−46.239 (9)	−386 (10)
0.70	45.561 (9)	−0.77 (2)	−45.854 (8)	−342 (10)
0.80	49.79 (1)	−0.58 (3)	−45.073 (7)	−243 (9)
0.85	51.93 (1)	−0.45 (3)	−44.671 (8)	−182 (11)
0.90	54.07 (1)	−0.33 (3)	−44.292 (7)	−145 (10)
1	58.44 (1)		−43.465 (8)	